Stochastic Networks in Nanoscale Biophysics: Modeling Enzymatic Reaction of a Single Protein

S. C. KOU

Advances in nanotechnology enable scientists for the first time to study biological processes on a nanoscale molecule-by-molecule basis. A surprising discovery from recent nanoscale single-molecule biophysics experiments is that biological reactions involving enzymes behave fundamentally differently from what classical theory predicts. In this article we introduce a stochastic network model to explain the experimental puzzles (by modeling enzymatic reactions as a stochastic network connected by different enzyme conformations). Detailed analyses of the model, including analyses of the first-passage-time distributions and goodness of fit, show that the stochastic network model is capable of explaining the experimental surprises. The model is analytically tractable and closely fits experimental data. The biological/chemical meaning of the model is discussed.

KEY WORDS: Autocorrelation function; Continuous-time Markov chain; First passage time; Goodness of fit; Maximum likelihood estimates; Michaelis–Menten model; Reaction rate.

1. INTRODUCTION

The rapid advances in nanotechnology have generated much excitement in the scientific and engineering communities. Its application to the biological front in the last two decades led to the new field of nanoscale biophysics: Scientists for the first time were able to study biological processes on an unprecedented nanoscale molecule-by-molecule basis (Nie and Zare 1997; Xie and Trautman 1998; Xie and Lu 1999; Tamarat, Maali, Lounis, and Orrit 2000; Weiss 2000; Moerner 2002; Kou, Xie, and Liu 2005b). This new development has opened the door to addressing many problems that were inaccessible just a few decades ago and has attracted much attention from biologists, chemists, and biophysicists, because nanoscale *single-molecule* experiments offer many advantages over the traditional experiments involving a *population* of molecules. First, by allowing scientists to "zoom in" on individual molecules, single-molecule experiments provide data with more accuracy and higher resolution. Second, by isolating, tracking, and manipulating individual molecules, single-molecule experiments capture transient intermediates and detailed dynamics of a biological process, the type of information rarely available from traditional population experiments. Third, by following single molecules, scientists can study biological processes directly on the individual molecule level, instead of relying on the extremely difficult task of synchronizing the actions of a population of biomolecules. Fourth, because many important biological functions in a living cell are performed by single molecules, understanding the behavior of individual biomolecules is a crucial task, for which single-molecule experiments are specifically designed. Many new scientific discoveries (see, e.g., Lu, Xun, and Xie 1998; Zhuang et al. 2002; Asbury, Fehr, and Block 2003; Yang et al. 2003; Kou and Xie 2004; Kou et al. 2005a) have emerged from the nanoscale single-molecule studies.

Advances in nanoscale single-molecule biophysics also bring opportunities for statisticians and probabilists because to characterize the behavior of individual molecules, which exist in the nanometer world subject to the laws of statistical and quantum mechanics, stochastic models and their statistical inference are indispensable (Kou 2008).

In this article we consider recent single-molecule experiments on enzymatic reactions (Flomembom et al. 2005; English et al. 2006), where the high-resolution experimental results showed a surprising departure from what classical theory predicts. To explain the single-molecule experimental findings, we introduce a stochastic network model to describe the enzymatic reaction kinetics.

According to the classical Michaelis–Menten (MM) model of enzymatic reaction in biochemistry (Atkins and de Paula 2002), an enzyme catalyzes a reaction in the following way. First, the enzyme binds to the reactant, which is referred to in the biochemistry literature as a substrate, and forms an enzyme–substrate complex. The complex then undergoes a decomposition to generate the reaction product and release the enzyme in its original form to catalyze the next substrate. In the biochemistry literature this process is typically diagrammed as

$$E + S \rightleftarrows ES \to E^0 + P, \qquad E^0 \to E,$$

where the arrows indicate the reaction direction and E (and E^0), S, ES, and P stand for the enzyme, the substrate, the enzyme–substrate complex, and the reaction product, respectively.

In addition to providing a schematic picture, the classical MM model also gives quantitative results; for example, it explicitly describes how the reaction rate depends on the substrate concentration (see Sec. 2 for details). Over the years, numerous experiments carried out in the traditional way (i.e., using a population of enzymes and substrates) yielded results agreeing with the quantitative descriptions of the MM model, and, thus, for decades the MM model was featured in textbooks as the fundamental mechanism for enzymatic reactions (Hammes 1982; Fersht 1985; Segel 1993).

Recent nanoscale single-molecule experiments (English et al. 2006), which for the first time tracked the behavior of a single enzyme, however, have surprised researchers, as the high-resolution experimental data showed an unequivocal departure from the MM model:

S. C. Kou is John L. Loeb Associate Professor of the Natural Sciences, Department of Statistics, Harvard University, Cambridge, MA 02138 (E-mail: *kou@stat.harvard.edu*). The author thanks the Xie group of the Department of Chemistry and Chemical Biology of Harvard University for sharing the experimental data and for fruitful discussions. The research was supported in part by NSF Career Award DMS-0449204.

© 2008 American Statistical Association
Journal of the American Statistical Association
September 2008, Vol. 103, No. 483, Applications and Case Studies
DOI 10.1198/016214507000001021

- First, under the MM model a single enzyme behaves as a continuous-time Markov chain, switching among the three states E, ES, and E^0. From the Markov description, the MM model predicts that an enzyme's turnover time, which is the time that it takes the enzyme to complete one catalytic cycle (i.e., to go from state E to state E^0), should have (almost) a purely exponential distribution. The single-molecule experimental data, however, show that the distribution of the turnover time is actually much heavier than an exponential one.
- Second, because under the MM model a single enzyme behaves as a continuous-time Markov chain, it follows from the Markov property that an enzyme's successive turnover times should be independently and identically distributed. In the single-molecule experiments, however, it is observed that a single enzyme's successive turnover times are, in fact, highly correlated, possessing a strong memory.
- Third, the MM model gives a formula (known as the Michaelis–Menten equation in the literature) that displays a hyperbolic relationship between the reaction rate and the substrate concentration. This formula appears to hold for the single-molecule experimental data.

Sections 2 and 5 will provide more details. Some questions immediately arise from these observations. First, what causes the turnover time's heavier-than-exponential distribution? Second, how can an enzyme "remember" its past, and from where does the memory come? Third, given that the experimental data have contradicted the two fundamental predictions of the MM model, how can the explicit formula derived from the MM equation still hold?

We formulate a stochastic network model to answer these questions.

From a statistics standpoint, we conduct a detailed analysis of the stochastic network: studying its statistical inference as well as analyzing the first passage times on the network, as both are crucial in explaining the experimental puzzles.

From an application point of view, we show that by utilizing a stochastic network structure to describe enzymatic reaction kinetics at the molecular level, the recent experimental puzzles can be satisfactorily resolved.

The outline of the article is as follows. Section 2 reviews the experimental puzzles that motivate our study and introduces our stochastic network model; special attention is paid to the biological/chemical meaning of the model components. Section 3 investigates the properties of the model, the stationary and the first-passage-time distributions in particular. The analytical results are applied in Section 4 to explain the experimental puzzles. Section 5 considers data from recent single-molecule experiments, assesses the goodness of fit of the MM model to the real data, and uses maximum likelihood to fit our model to the experimental data, showing close agreement between our model and the data. Section 6 concludes the article with a discussion. All the technical derivations and proofs are given in the Appendix.

2. MODELING ENZYMATIC REACTIONS

2.1 The Classical Michaelis–Menten Model and Its Limitations

To facilitate the introduction of our model, we first review the classical MM model and its limitations in explaining recent single-molecule experimental results.

In the MM model, with the substrate concentration held constant, a single enzyme molecule cycles repetitively through the three states E, ES, and E^0 via

$$E + S \underset{k_{-1}}{\overset{k_1[S]}{\rightleftarrows}} ES \overset{k_2}{\to} E^0 + P, \qquad E^0 \overset{\delta}{\to} E, \tag{2.1}$$

where the symbol $[S]$ denotes the (constant) substrate concentration; k_1 is the association rate (per unit substrate concentration); k_{-1} and k_2 are, respectively, the dissociation and catalytic rate; and δ is the rate of E^0's return to E.

In our familiar statistics language, diagram (2.1) is the routing map of a three-state continuous-time Markov chain with the infinitesimal generator (transition matrix)

$$\mathbf{Q}_{\mathrm{MM}} = \begin{pmatrix} -k_1[S] & k_1[S] & 0 \\ k_{-1} & -(k_{-1}+k_2) & k_2 \\ \delta & 0 & -\delta \end{pmatrix}.$$

An enzyme molecule switches continuously among the three states E, ES, and E^0 according to $\mathbf{Q}_{\mathrm{MM}}$.

The time needed for an enzyme to complete one catalytic cycle is called the *turnover time*.

In the MM model the turnover time is the first passage time from state E to state E^0. The density function of this first passage time is given by the following proposition, whose derivation is deferred to the Appendix.

Proposition 2.1. The density function of the first passage time from state E to state E^0 is

$$f(t) = \frac{k_1 k_2 [S]}{2p}\left(e^{-(q-p)t} - e^{-(q+p)t}\right), \tag{2.2}$$

where $p = \sqrt{(k_1[S]+k_2+k_{-1})^2/4 - k_1 k_2 [S]}$ and $q = (k_1[S]+k_2+k_{-1})/2$.

Equation (2.2), together with (2.1), has important experimental implications for the MM model.

- First, (2.2) says that the distribution of the turnover time should have an exponential decay with rate $q-p$ in the MM model. Furthermore, due to the exponential nature, for most values of t, $e^{-(q-p)t}$ easily overwhelms $e^{-(q+p)t}$; thus, $f(t)$ is almost a purely exponential distribution, and will, thus, yield a practically straight line on a log-linear plot. Figure 1 illustrates this point, plotting $f(t)$ on a log-linear scale for typical values of $[S]$, k_1, k_2, and k_{-1}; a clear linear pattern is shown.
- Second, because an enzyme's behavior is modeled as a Markov chain in the MM model, it follows immediately that an enzyme's successive turnover times are independently and identically distributed. No memory should be found among the turnover times.

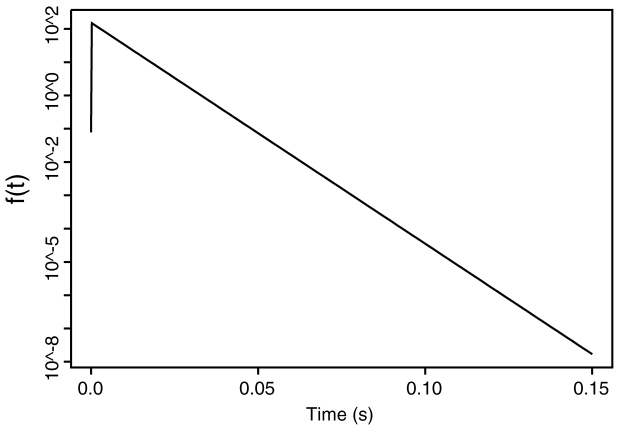

Figure 1. Density function $f(t)$ of the turnover time from the MM model plotted on a log-linear scale. $[S] = 100$ μM (micromolar), $k_1 = 5 \times 10^7$ M^{-1} s^{-1}, $k_2 = 730$ s^{-1}, $k_{-1} = 18{,}300$ s^{-1}.

- Third, from (2.2) we know that the mean turnover time is

$$\int_0^\infty f(t)t\,dt = \frac{k_1[S] + k_2 + k_{-1}}{k_1 k_2 [S]}.$$

The reciprocal of the mean turnover time is defined as the enzymatic *reaction rate* (Yang and Cao 2001; Kou et al. 2005a; Min et al. 2006):

$$v = 1\Big/\left(\int_0^\infty f(t)t\,dt\right) = \frac{k_2[S]}{[S] + (k_2 + k_{-1})/k_1}. \quad (2.3)$$

This relationship, referred to as the Michaelis–Menten equation, is of fundamental importance in the biochemistry literature (Segel 1993; Atkins and de Paula 2002): It gives an explicit hyperbolic dependence of the reaction rate v on the substrate concentration $[S]$.

Before nanoscale single-molecule experiments were possible, numerous researchers had studied different enzyme systems under the traditional experimental approach. Unable to follow an individual enzyme molecule, the traditional experiments relied on a population of enzymes, and by measuring the accumulation of reaction products over time, researchers estimated the reaction rate for various substrate concentrations. It was found in these traditional experiments that the hyperbolic form in (2.3), that is,

$$v \propto [S]/([S] + C) \quad \text{with some constant } C,$$

appeared to hold for many enzymes. Thus, for decades the MM model has been featured in textbooks as the fundamental mechanism for enzymatic reactions (Hammes 1982; Fersht 1985; Segel 1993).

Advances in nanotechnology have made it possible to study enzymatic reactions at the single-molecule level. English et al. (2006) recently carried out single-molecule experiments to study β-galactosidase, an essential enzyme in the human body that catalyzes the breakdown of the sugar lactose (Jacobson, Zhang, DuBose, and Matthews 1994; Dorland 2003). The experimental results surprised researchers, as the high-resolution data clearly demonstrated that

a. The empirical distribution of the experimentally recorded turnover times is much heavier than an exponential one.

b. A single enzyme's successive turnover times are strongly correlated.

c. The hyperbolic relationship of $v \propto [S]/([S] + C)$ appears to hold true for the single-molecule data.

Section 5 will provide details about the experiments. Given that findings (a) and (b) contradict the fundamentals of the MM model, finding (c) is even more surprising.

2.2 The Stochastic Network Model

Model Construction. An important clue in our effort to resolve the experimental puzzles comes from other recent single-molecule experiments (Lu et al. 1998; Yang et al. 2003; Kou and Xie 2004; Min et al. 2005a; Min et al. 2005b), where, in studying different biological systems, researchers have become aware that enzymes are not rigid entities but rather *dynamic* biomolecules, experiencing constant changes and fluctuations in their three-dimensional shape and configuration. This observation suggests that we should not treat an enzyme as an object with a fixed state; instead, we should view an enzyme as a collection of states, each state being a distinct conformation (i.e., a distinct spatial configuration) with an enzyme spontaneously switching among the different states. With this insight we propose the following stochastic network model for enzymatic reactions, diagrammed as

$$\begin{array}{ccccc}
S + E_1 & \underset{k_{-11}}{\overset{k_{11}[S]}{\rightleftarrows}} & ES_1 & \overset{k_{21}}{\to} P + E_1^0, & E_1^0 \overset{\delta_1}{\to} E_1, \\
\downarrow\uparrow & & \downarrow\uparrow & \downarrow\uparrow & \vdots \\
S + E_2 & \underset{k_{-12}}{\overset{k_{12}[S]}{\rightleftarrows}} & ES_2 & \overset{k_{22}}{\to} P + E_2^0, & E_2^0 \overset{\delta_2}{\to} E_2, \\
\vdots & & \vdots & \vdots & \vdots \\
\downarrow\uparrow & & \downarrow\uparrow & \downarrow\uparrow & \\
S + E_n & \underset{k_{-1n}}{\overset{k_{1n}[S]}{\rightleftarrows}} & ES_n & \overset{k_{2n}}{\to} P + E_n^0, & E_n^0 \overset{\delta_n}{\to} E_n,
\end{array} \quad (2.4)$$

where $E_1, E_2, \ldots$ represent the different states (conformations) of the original enzyme, and ES_i and E_i^0 are the states corresponding to subsequent enzyme–substrate binding and decomposition. The parameter $[S]$ in (2.4) denotes the concentration of substrate [as in (2.1)]; k_{1i} is the association rate (per unit concentration) for the ith state E_i; and k_{-1i}, k_{2i}, and δ_i are, respectively, the dissociation, catalytic, and returning rates corresponding to the transitions from ES_i to $S + E_i$, from ES_i to $P + E_i^0$, and from E_i^0 to E_i, respectively.

The transitions among the E_i's in the model capture the (conformational) fluctuation of the enzyme. It should be understood that E_i not only connects with E_{i-1} and E_{i+1} but also with all the other E_j's [we only depict the $E_i \leftrightarrow E_{i-1}$ and $E_i \leftrightarrow E_{i+1}$ transitions in (2.4) due to graphical limitations], and the same is true among the ES_i states and the E_i^0 states, respectively.

Different states, due to their specific spatial arrangement, could have different reactivity levels. This is embodied in the model by allowing k_{1i}, k_{-1i}, k_{2i}, and δ_i to take distinct values for different i.

The transitions between $S + E_i$ and ES_i incorporate the insight that in a real enzymatic reaction, the enzyme–substrate binding should take place between the substrate and a specific spatial configuration of the enzyme (and in this regard there is

no transition between $S + E_i$ and ES_j and between ES_i and E_j^0 for $i \neq j$ because they correspond to different conformations).

Our model (2.4) generalizes the classical MM model to a stochastic network in the sense of Kelly and Williams (1995), Glasserman, Sigman, and Yao (1996), Chen and Yao (2001), and Ball, Kurtz, Popovic, and Rempala (2006). Each stage of enzymatic reaction (initiation, binding, and decomposition) consists of a collection of states (enzyme conformations). As we shall see, this multistates network structure plays a central role in explaining the experimental results.

Statistical Formulation. Let α_{ij} denote the transition rate from E_i to E_j ($i \neq j$), β_{ij} denote the transition rate from ES_i to ES_j, and γ_{ij} denote the transition rate from E_i^0 to E_j^0. Then the stochastic network (2.4) can be described as a continuous-time Markov chain with infinitesimal generator (transition matrix)

$$\mathbf{Q} = \begin{pmatrix} \mathbf{Q}_{AA} - \mathbf{Q}_{AB} & \mathbf{Q}_{AB} & \mathbf{0} \\ \mathbf{Q}_{BA} & \mathbf{Q}_{BB} - (\mathbf{Q}_{BA} + \mathbf{Q}_{BC}) & \mathbf{Q}_{BC} \\ \mathbf{Q}_{CA} & \mathbf{0} & \mathbf{Q}_{CC} - \mathbf{Q}_{CA} \end{pmatrix}, \tag{2.5}$$

where for notational convenience the square matrix $\mathbf{Q}_{AA}$ represents the transition rates among the E_i states (think of A_i as shorthand notation for E_i),

$$(\mathbf{Q}_{AA})_{ij} = \alpha_{ij} \quad \text{for } i \neq j, \qquad (\mathbf{Q}_{AA})_{ii} = -\sum_{j \neq i} \alpha_{ij}.$$

Likewise, the matrices $\mathbf{Q}_{BB}$ and $\mathbf{Q}_{CC}$ represent the transition rates among the ES_i states and E_i^0 states, respectively (think of B_i and C_i as shorthand notation for ES_i and E_i^0, respectively),

$$(\mathbf{Q}_{BB})_{ij} = \beta_{ij} \quad \text{for } i \neq j, \qquad (\mathbf{Q}_{BB})_{ii} = -\sum_{j \neq i} \beta_{ij},$$

$$(\mathbf{Q}_{CC})_{ij} = \gamma_{ij} \quad \text{for } i \neq j, \qquad (\mathbf{Q}_{CC})_{ii} = -\sum_{j \neq i} \gamma_{ij}.$$

The diagonal matrices $\mathbf{Q}_{AB}$, $\mathbf{Q}_{BA}$, $\mathbf{Q}_{BC}$, and $\mathbf{Q}_{CA}$ in (2.5) denote the transition rates from E_i to ES_i, from ES_i to E_i, from ES_i to E_i^0, and from E_i^0 to E_i, respectively: $\mathbf{Q}_{AB} = \operatorname{diag}(k_{11}[S], k_{12}[S], \ldots, k_{1n}[S])$, $\mathbf{Q}_{BA} = \operatorname{diag}(k_{-11}, k_{-12}, \ldots, k_{-1n})$, $\mathbf{Q}_{BC} = \operatorname{diag}(k_{21}, k_{22}, \ldots, k_{2n})$, and $\mathbf{Q}_{CA} = \operatorname{diag}(\delta_1, \delta_2, \ldots, \delta_n)$.

Turnover Time. In our model (2.4) an enzyme's turnover time is the first passage time from the first reaction stage to the third stage, that is, from any E_i state to any E_j^0 state. For example, suppose an enzyme travels through the following path: $E_1^0 \to E_1 \to E_2 \to ES_2 \to E_2^0 \to E_2 \to E_3 \to ES_3 \to ES_1 \to S_1 \to ES_1 \to E_1^0$. Then the first turnover time corresponds to $E_1 \to E_2 \to ES_2 \to E_2^0$, and the second corresponds to $E_2 \to E_3 \to ES_3 \to ES_1 \to S_1 \to ES_1 \to E_1^0$. The feature that a turnover event can start from any E_i and end in any E_j^0 in our model captures the fact that in a single-molecule experiment, instead of observing the specific enzyme conformations and their interconversions, one can record only the time for an enzyme to complete a reaction cycle. In other words, on the network (2.4), the exact states are not observed, and only transitions from the first stage (consisting of $E_1, \ldots, E_n$) to the last stage (consisting of $E_1^0, \ldots, E_n^0$) are observed.

3. PROPERTIES OF THE STOCHASTIC NETWORK MODEL

We study the stochastic network model in this section. The results will be used in Section 4 to explain the experimental puzzles.

3.1 Detailed Balance: A Constraint on the Model

An important chemical requirement for kinetic models is the detailed balance condition (Lewis 1925; Schnakenberg 1976; Kelly 1979). It states that if any two states are *mutually* spontaneously convertible, then detailed balance must hold between them. In our case, because E_i and E_j are mutually convertible, and so are the pairs ES_i and ES_j, E_i^0, and E_j^0, and E_i and ES_i, the transition rates must satisfy the following constraints: There exist positive numbers $\phi(E_i)$, $\phi(ES_i)$, and $\phi(E_i^0)$ ($i = 1, 2, \ldots, n$) such that, for any i and j,

$$\begin{aligned} &\phi(E_i)\alpha_{ij} = \phi(E_j)\alpha_{ji}, \qquad \phi(ES_i)\beta_{ij} = \phi(ES_j)\beta_{ji}, \\ &\phi(E_i)k_{1i}[S] = \phi(ES_i)k_{-1i}, \qquad \phi(E_i^0)\gamma_{ij} = \phi(E_j^0)\gamma_{ji}. \end{aligned} \tag{3.1}$$

In matrix notation the detailed balance condition can be concisely written as

$$\begin{aligned} &\begin{pmatrix} \mathbf{\Phi}_A & \mathbf{0} \\ \mathbf{0} & \mathbf{\Phi}_B \end{pmatrix} \begin{pmatrix} \mathbf{Q}_{AA} & \mathbf{Q}_{AB} \\ \mathbf{Q}_{BA} & \mathbf{Q}_{BB} \end{pmatrix} \\ &\quad = \begin{pmatrix} \mathbf{Q}_{AA} & \mathbf{Q}_{AB} \\ \mathbf{Q}_{BA} & \mathbf{Q}_{BB} \end{pmatrix}^T \begin{pmatrix} \mathbf{\Phi}_A & \mathbf{0} \\ \mathbf{0} & \mathbf{\Phi}_B \end{pmatrix}, \\ &\mathbf{\Phi}_C \mathbf{Q}_{CC} = \mathbf{Q}_{CC}^T \mathbf{\Phi}_C, \end{aligned} \tag{3.2}$$

where the diagonal matrices $\mathbf{\Phi}_A = \operatorname{diag}(\phi(E_1), \phi(E_2), \ldots, \phi(E_n))$, $\mathbf{\Phi}_B = \operatorname{diag}(\phi(ES_1), \ldots, \phi(ES_n))$, and $\mathbf{\Phi}_C = \operatorname{diag}(\phi(E_1^0), \ldots, \phi(E_n^0))$.

The detailed balance condition (3.1) implies, in particular, that if we isolate the E_i states ($i = 1, 2, \ldots, n$) and look only at transitions among them, that is, if we look at the subnetwork of (2.5) with transition matrix $\mathbf{Q}_{AA}$, then

$$\boldsymbol{\phi}_A = \big(\phi(E_1), \phi(E_2), \ldots, \phi(E_n)\big) \tag{3.3}$$

is the stationary measure for the subnetwork: $\boldsymbol{\phi}_A \mathbf{Q}_{AA} = 0$. Similarly, for ES_i states in isolation, and E_i^0 states in isolation

$$\begin{aligned} &\boldsymbol{\phi}_B = \big(\phi(ES_1), \ldots, \phi(ES_n)\big) \qquad \text{and} \\ &\boldsymbol{\phi}_C = \big(\phi(E_1^0), \ldots, \phi(E_n^0)\big) \end{aligned} \tag{3.4}$$

are the stationary measures for the subnetworks, respectively: $\boldsymbol{\phi}_B \mathbf{Q}_{BB} = 0$, $\boldsymbol{\phi}_C \mathbf{Q}_{CC} = 0$. Furthermore, if we consider the subnetwork consisting of E_i and ES_i states ($i = 1, 2, \ldots, n$) together [which has $\begin{pmatrix} \mathbf{Q}_{AA} - \mathbf{Q}_{AB} & \mathbf{Q}_{AB} \\ \mathbf{Q}_{BA} & \mathbf{Q}_{BB} - \mathbf{Q}_{BA} \end{pmatrix}$ as the transition matrix], $(\boldsymbol{\phi}_A, \boldsymbol{\phi}_B)$ is the stationary measure:

$$(\boldsymbol{\phi}_A, \boldsymbol{\phi}_B) \begin{pmatrix} \mathbf{Q}_{AA} - \mathbf{Q}_{AB} & \mathbf{Q}_{AB} \\ \mathbf{Q}_{BA} & \mathbf{Q}_{BB} - \mathbf{Q}_{BA} \end{pmatrix} = 0.$$

On the other hand, because ES_i and E_i^0 are not mutually convertible, there is no detailed balance between them, and, in general, $(\boldsymbol{\phi}_A, \boldsymbol{\phi}_B, \boldsymbol{\phi}_C)$ is *not* the stationary measure of the entire network: $(\boldsymbol{\phi}_A, \boldsymbol{\phi}_B, \boldsymbol{\phi}_C)\mathbf{Q} \neq 0$.

Remark 1. It is worth emphasizing that in our model detailed balance holds only for subnetworks, not for the entire network. The reason is that (1) the transition rate k_{2i} from ES_i to E_i^0 is positive, but there is no transition from E_i^0 to ES_i, and (2) the transition rate δ_i from E_i^0 to E_i is positive, but there is no transition from E_i to E_i^0. Therefore, there do not exist nonzero $\phi(E_i)$, $\phi(ES_i)$, and $\phi(E_i^0)$ to maintain the detailed balance between ES_i and E_i^0 or between E_i and E_i^0. From a chemical standpoint, this happens because ES_i and E_i^0 (and E_i and E_i^0) are not *mutually* spontaneously convertible. Except for these special pairs, the detailed balance, however, does hold for any other pairs; for example, it holds between E_i and E_j, between ES_i and ES_j, between E_i^0 and E_j^0, and between E_i and ES_i as shown in (3.1).

3.2 Stationary Distribution

Let $X(t)$ be the process evolving according to our stochastic network model (2.4).

Lemma 3.1. Suppose all the parameters $k_{1i}, k_{-1i}, k_{2i}, \delta_i, \alpha_{ij}, \beta_{ij}$, and γ_{ij} are positive. Then the continuous-time Markov chain $X(t)$ is ergodic. Let the row vectors $\boldsymbol{\pi}_A = (\pi(E_1), \pi(E_2), \ldots, \pi(E_n))$, $\boldsymbol{\pi}_B = (\pi(ES_1), \ldots, \pi(ES_n))$, and $\boldsymbol{\pi}_C = (\pi(E_1^0), \ldots, \pi(E_n^0))$ denote the stationary distribution of the entire network. Up to a normalizing constant, they are determined by

$$\boldsymbol{\pi}_A = -\boldsymbol{\pi}_C \mathbf{Q}_{CA}\mathbf{L}, \qquad \boldsymbol{\pi}_B = -\boldsymbol{\pi}_C \mathbf{Q}_{CA}\mathbf{M}, \tag{3.5}$$

$$\boldsymbol{\pi}_C(\mathbf{Q}_{CC} - \mathbf{Q}_{CA} - \mathbf{Q}_{CA}\mathbf{M}\mathbf{Q}_{BC}) = 0, \tag{3.6}$$

where the matrices $\mathbf{L}$ and $\mathbf{M}$ are given by

$$\mathbf{L} = [\mathbf{Q}_{AA} - \mathbf{Q}_{AB} - \mathbf{Q}_{AB}(\mathbf{Q}_{BB} - \mathbf{Q}_{BA} - \mathbf{Q}_{BC})^{-1}\mathbf{Q}_{BA}]^{-1}, \tag{3.7}$$

$$\mathbf{M} = [\mathbf{Q}_{BB} - \mathbf{Q}_{BC} - (\mathbf{Q}_{BB} - \mathbf{Q}_{BA} - \mathbf{Q}_{BC})\mathbf{Q}_{AB}^{-1}\mathbf{Q}_{AA}]^{-1}. \tag{3.8}$$

Lemma 3.1, whose derivation is deferred to the Appendix, tells us that to obtain the stationary measure of $X(t)$, the key equation is (3.6) because upon solving it for $\boldsymbol{\pi}_C$ we can immediately get $\boldsymbol{\pi}_A$ and $\boldsymbol{\pi}_B$ via (3.5).

3.3 Distributions of First Passage Times

As we noted in Section 2.2, an enzyme turnover event in our model can start from any E_i state and end in any E_j^0 state. To calculate the turnover time distributions, let T_{E_i} and T_{ES_i} denote the first passage time to reach the set $\{E_1^0, \ldots, E_n^0\}$ from states E_i and ES_i, respectively, and let $f_{E_i}(t)$ and $f_{ES_i}(t)$ be their corresponding density functions. The following theorem provides an explicit formula for the distributions in terms of their Laplace transforms.

Theorem 3.2. Let $\tilde{f}_{E_i}(s)$ and $\tilde{f}_{ES_i}(s)$ be the Laplace transforms of $f_{E_i}(t)$ and $f_{ES_i}(t)$ [i.e., $\tilde{f}_J(s) = \int_0^\infty e^{-st} f_J(t)\,dt$, $J = E_i$ or ES_i] and denote $\tilde{\mathbf{f}}_A(s) = (\tilde{f}_{E_1}(s), \tilde{f}_{E_2}(s), \ldots, \tilde{f}_{E_n}(s))^T$ and $\tilde{\mathbf{f}}_B(s) = (\tilde{f}_{ES_1}(s), \tilde{f}_{ES_2}(s), \ldots, \tilde{f}_{ES_n}(s))^T$. Then the distributions of the turnover times are given by

$$\begin{pmatrix} \tilde{\mathbf{f}}_A(s) \\ \tilde{\mathbf{f}}_B(s) \end{pmatrix} = \left[s\mathbf{I} - \begin{pmatrix} \mathbf{Q}_{AA} - \mathbf{Q}_{AB} & \mathbf{Q}_{AB} \\ \mathbf{Q}_{BA} & \mathbf{Q}_{BB} - \mathbf{Q}_{BA} - \mathbf{Q}_{BC} \end{pmatrix} \right]^{-1} \times \begin{pmatrix} \mathbf{0} \\ \mathbf{Q}_{BC}\mathbf{1} \end{pmatrix}, \tag{3.9}$$

where the boldface $\mathbf{1}$ denotes the vector $(1, 1, \ldots, 1)^T$.

The derivation of Theorem 3.2 is given in the Appendix. The following corollary is a direct consequence of Theorem 3.2; its proof is also deferred to the Appendix.

Corollary 3.3. Let the vectors $\boldsymbol{\mu}_A = (E(T_{E_1}), E(T_{E_2}), \ldots, E(T_{E_n}))^T$ and $\boldsymbol{\mu}_B = (E(T_{ES_1}), \ldots, E(T_{ES_n}))^T$ denote the mean first passage times. Then they are given by

$$\begin{pmatrix} \boldsymbol{\mu}_A \\ \boldsymbol{\mu}_B \end{pmatrix} = \begin{pmatrix} -(\mathbf{L} + \mathbf{M})\mathbf{1} \\ -(\mathbf{N} + \mathbf{R})\mathbf{1} \end{pmatrix}, \tag{3.10}$$

where the matrices $\mathbf{L}$ and $\mathbf{M}$ are defined in Lemma 3.1, and the matrices $\mathbf{N}$ and $\mathbf{R}$ are given by

$$\mathbf{N} = [\mathbf{Q}_{AA} - (\mathbf{Q}_{AA} - \mathbf{Q}_{AB})\mathbf{Q}_{BA}^{-1}(\mathbf{Q}_{BB} - \mathbf{Q}_{BC})]^{-1},$$

$$\mathbf{R} = [\mathbf{Q}_{BB} - \mathbf{Q}_{BA} - \mathbf{Q}_{BC} - \mathbf{Q}_{BA}(\mathbf{Q}_{AA} - \mathbf{Q}_{AB})^{-1}\mathbf{Q}_{AB}]^{-1}.$$

3.4 Stationary Turnover Time Distribution and Reaction Rate

A single-molecule experiment tracks the reaction cycles of a single enzyme, records the enzyme's successive turnover times over a long period, and then obtains the empirical distribution (i.e., the histogram) of these recorded turnover times. To find the theoretical correspondence of this empirical distribution, we first note that in our model a turnover event can start from any state E_i, each having its own first-passage-time distribution $f_{E_i}(t)$. Therefore, in the long run, the *overall* distribution of *all* the turnover times should be characterized by the weighted average of $f_{E_i}(t)$ with the weights given by the stationary probability of a turnover event's starting from E_i. Let $w(E_i)$ denote this stationary probability; the overall stationary (equilibrium) turnover time distribution is then

$$f_{\text{eq}}(t) = \sum_i w(E_i) f_{E_i}(t).$$

Lemma 3.4. The Laplace transform $\tilde{f}_{\text{eq}}(s)$ of $f_{\text{eq}}(t)$ is

$$\tilde{f}_{\text{eq}}(s) = \frac{\mathbf{w}\tilde{\mathbf{f}}_A(s)}{\mathbf{w}\mathbf{1}},$$

where the (row) weighting vector $\mathbf{w}$, up to a normalizing constant, is the nonzero solution of

$$\mathbf{w}(\mathbf{I} + \mathbf{M}\mathbf{Q}_{BC} - \mathbf{Q}_{CA}^{-1}\mathbf{Q}_{CC}) = 0, \tag{3.11}$$

and $\tilde{\mathbf{f}}_A(s)$ is given in Theorem 3.2 (the matrix $\mathbf{M}$ is defined in Lemma 3.1).

Combining the results of Corollary 3.3 and Lemma 3.4, we have the following result.

Corollary 3.5. The mean stationary turnover time under model (2.4) is given by

$$\begin{aligned}\mu_{\text{eq}} &= \int_0^\infty t f_{\text{eq}}(t)\,dt \\ &= \frac{1}{\mathbf{w1}}\mathbf{w}(\mathbf{I}-\mathbf{Q}_{CA}^{-1}\mathbf{Q}_{CC})\mathbf{Q}_{BC}^{-1} \\ &\quad\times[\mathbf{I}-(\mathbf{Q}_{BB}-\mathbf{Q}_{BA}-\mathbf{Q}_{BC})\mathbf{Q}_{AB}^{-1}]\mathbf{1}, \qquad (3.12)\end{aligned}$$

where the row vector $\mathbf{w}$ is defined in Lemma 3.4.

Reaction Rate. The reciprocal of an enzyme's mean stationary turnover time is defined as the enzymatic reaction rate (Yang and Cao 2001; Kou et al. 2005a; Min et al. 2006). Therefore, under our stochastic network model (2.4), the reaction rate v is given by

$$\begin{aligned}v = 1/\mu_{\text{eq}} = \{\mathbf{w1}\}/\big\{&\mathbf{w}(\mathbf{I}-\mathbf{Q}_{CA}^{-1}\mathbf{Q}_{CC})\mathbf{Q}_{BC}^{-1} \\ &\times[\mathbf{I}-(\mathbf{Q}_{BB}-\mathbf{Q}_{BA}-\mathbf{Q}_{BC})\mathbf{Q}_{AB}^{-1}]\mathbf{1}\big\}.\end{aligned}$$

4. EXPLAINING THE EXPERIMENTAL PUZZLES

Utilizing the previous results, we now apply our model to explain the single-molecule experimental findings, starting from the first puzzle.

4.1 Heavier-Than-Exponential Turnover Time Distribution

The MM model predicts the turnover time distribution to be nearly exponential (see Sec. 2.1 and Fig. 1). This prediction, however, is contradicted by the single-molecule experimental finding that the empirical distribution of an enzyme's turnover times actually exhibits a heavily skewed right tail. (We will give details about the experiments in Sec. 5.) Our stochastic network model, on the other hand, offers a simple explanation.

As we noted in Section 3.4, the empirical turnover time distribution is theoretically characterized in our model by the stationary turnover time distribution $f_{\text{eq}}(t)$. Its Laplace transform, according to Lemma 3.4 and Theorem 3.2, is

$$\begin{aligned}\tilde{f}_{\text{eq}}(s) &= \frac{1}{\mathbf{w1}}\begin{pmatrix}\mathbf{w} & \mathbf{0}\end{pmatrix}\begin{pmatrix}\tilde{\mathbf{f}}_A(s)\\ \tilde{\mathbf{f}}_B(s)\end{pmatrix} \\ &= \frac{1}{\mathbf{w1}}\begin{pmatrix}\mathbf{w} & \mathbf{0}\end{pmatrix} \\ &\quad\times\left[s\mathbf{I}-\begin{pmatrix}\mathbf{Q}_{AA}-\mathbf{Q}_{AB} & \mathbf{Q}_{AB}\\ \mathbf{Q}_{BA} & \mathbf{Q}_{BB}-\mathbf{Q}_{BA}-\mathbf{Q}_{BC}\end{pmatrix}\right]^{-1} \\ &\quad\times\begin{pmatrix}\mathbf{0}\\ \mathbf{Q}_{BC}\mathbf{1}\end{pmatrix}, \qquad (4.1)\end{aligned}$$

where the weighting vector $\mathbf{w}$ is defined in (3.11). The next lemma simplifies this expression.

Lemma 4.1. Let $\mathbf{G}$ denote the matrix

$$\begin{pmatrix}\mathbf{Q}_{AA}-\mathbf{Q}_{AB} & \mathbf{Q}_{AB}\\ \mathbf{Q}_{BA} & \mathbf{Q}_{BB}-\mathbf{Q}_{BA}-\mathbf{Q}_{BC}\end{pmatrix}.$$

It is diagonalizable:

$$\mathbf{G}=\mathbf{U}\boldsymbol{\Lambda}\mathbf{U}^{-1}=\sum_{i=1}^{2n}\lambda_i\boldsymbol{\xi}_i\boldsymbol{\eta}_i^T,$$

where the diagonal matrix $\boldsymbol{\Lambda}=\operatorname{diag}(\lambda_1,\lambda_2,\ldots,\lambda_{2n})$ consists of the eigenvalues of $\mathbf{G}$, which are strictly negative, the columns $\boldsymbol{\xi}_1,\boldsymbol{\xi}_2,\ldots,\boldsymbol{\xi}_{2n}$ of the matrix $\mathbf{U}$ are the right eigenvectors of $\mathbf{G}$, and the rows $\boldsymbol{\eta}_1^T,\boldsymbol{\eta}_2^T,\ldots,\boldsymbol{\eta}_{2n}^T$ of $\mathbf{U}^{-1}$ are the left eigenvectors. This diagonalization implies that

$$\tilde{f}_{\text{eq}}(s)=\sum_{i=1}^{2n}\sigma_i\frac{-\lambda_i}{s-\lambda_i},$$

where

$$\sigma_i=\frac{1}{-\lambda_i}\left[\frac{(\mathbf{w}\ \mathbf{0})\boldsymbol{\xi}_i}{\mathbf{w1}}\boldsymbol{\eta}_i^T\begin{pmatrix}\mathbf{0}\\ \mathbf{Q}_{BC}\mathbf{1}\end{pmatrix}\right],$$

which translates to

$$f_{\text{eq}}(t)=\sum_{i=1}^{2n}\sigma_i(-\lambda_i e^{\lambda_i t}). \qquad (4.2)$$

The proof is deferred to the Appendix.

Lemma 4.1 tells us that under our stochastic network model the stationary turnover time distribution consists of a mixture of exponential distributions (because $\lambda_i<0$ for all i). Therefore, as long as there are multiple states (conformations) in the network ($n>1$), the distribution, in general, would be heavier than a single exponential one.

Equation (4.2), thus, gives an explanation of the first experimental surprise. In particular, it says that if one plots the empirical distribution (i.e., the histogram) of successive turnover times on a logarithmic scale, instead of observing a straight line indicating a single-exponential tail, one would find a line skewed to the right, which is exactly what has been observed in the single-molecule experiments (see Sec. 5).

Remark 2. The multistates structure plays a central role here. Without it, we would not be able to have a heavier-than-exponential distribution to account for the experimental observation.

4.2 Memory (Correlation) Between Successive Turnover Times

Under the classical MM model (2.1) the turnover times of an enzyme are independently and identically distributed. The single-molecule experimental discovery of correlation between an enzyme's successive turnover times contradicts this prediction. Our stochastic network model provides a natural explanation of this puzzle.

The key is that in our model an enzyme turnover event can start from any E_i states (which models the fact that a single-molecule experiment records only the time for an enzyme to complete a reaction cycle and cannot observe the specific enzyme states; see Sec. 2.2). The unobservability of individual states gives rise to an aggregation effect: Rather than the detailed movements on the full network, one is able to observe only transitions from one group of states $\{E_1,\ldots,E_n\}$ to another group $\{E_1^0,\ldots,E_n^0\}$. The aggregation masks the original Markov structure and directly leads to correlation between successive turnover times.

To make the idea transparent, imagine there are only two states E_1 and E_2 for illustration per se:

$$\begin{array}{ccccc} S+E_1 & \underset{k_{-11}}{\overset{k_{11}[S]}{\rightleftarrows}} & ES_1 & \overset{k_{21}}{\to} P+E_1^0, & E_1^0, \overset{\delta_1}{\to} E_1, \\ {\scriptstyle\alpha_{12}}\downarrow\uparrow{\scriptstyle\alpha_{21}} & & {\scriptstyle\beta_{12}}\downarrow\uparrow{\scriptstyle\beta_{21}} & {\scriptstyle\gamma_{12}}\downarrow\uparrow{\scriptstyle\gamma_{21}} & \vdots \\ S+E_2 & \underset{k_{-12}}{\overset{k_{12}[S]}{\rightleftarrows}} & ES_2 & \overset{k_{22}}{\to} P+E_2^0, & E_2^0 \overset{\delta_2}{\to} E_2. \end{array}$$

Suppose the transition rates α_{ij}, β_{ij}, and γ_{ij} are all small, meaning that the transitions between E_1 and E_2, between ES_1 and ES_2, and between E_1^0 and E_2^0 are all infrequent. Then it is easily seen that if a turnover event starts from E_1, it is highly likely that the next turnover event will also start from E_1; the same is true for turnover events starting from E_2. Now imagine furthermore that E_1 and E_2 have different reactivity levels; for example, the transitions between E_1 and ES_1, from ES_1 to E_1^0, and from E_1^0 to E_1 are all fast, while the transitions between E_2 and ES_2, from ES_2 to E_2^0, and from E_2^0 to E_2 are all slow. Then it is clear that a slow/fast turnover will likely be followed by another slow/fast turnover, naturally producing the correlation between successive turnover times.

Remark 3. We see from the preceding discussion that the apparent memory does not mean an enzyme can actually "remember" its past. In fact, it is the aggregation effect, that is, the (experimental) indistinguishability of the individual states, that generates the apparent memory. In a similar spirit, this type of aggregate Markov process has been applied in the study of ion channels (see Colquhoun and Hawkes 1981; Fredkin and Rice 1986). The multistates structure again plays a pivotal role here. Without the multiple states, we would not have aggregation and, consequently, would not be able to account for the memory.

4.3 Hyperbolic Relationship Between Reaction Rate and Substrate Concentration

The classical MM model describes a hyperbolic dependence of the reaction rate v on the substrate concentration $[S]$ [see (2.3)]. Interestingly, in both traditional population-based experiments and recent single-molecule experiments, the hyperbolic relationship of $v \propto [S]/([S]+C)$ appears to hold. With the previous negative experimental results countering the MM model, a natural question is to make sense of this "positive" one. Our network model offers a resolution. In particular, it points out various general scenarios under which the hyperbolic form will arise.

The reaction rate in the network model was derived in Section 3.4 to be

$$v = \{\mathbf{w1}\}/\big\{\mathbf{w}(\mathbf{I}-\mathbf{Q}_{CA}^{-1}\mathbf{Q}_{CC})\mathbf{Q}_{BC}^{-1} \times [\mathbf{I}-(\mathbf{Q}_{BB}-\mathbf{Q}_{BA}-\mathbf{Q}_{BC})\mathbf{Q}_{AB}^{-1}]\mathbf{1}\big\}, \quad (4.3)$$

with the weighting vector $\mathbf{w}$ defined in (3.11). To find the link between v and $[S]$, we note that of all the transition rates in the model, only those from E_i to ES_i involve $[S]$: $\mathbf{Q}_{AB} = \mathrm{diag}(k_{11}[S], k_{12}[S], \ldots, k_{1n}[S])$. See Section 2.2. Let us denote

$$\mathbf{Q}_{AB} = [S]\tilde{\mathbf{Q}}_{AB}, \qquad \tilde{\mathbf{Q}}_{AB} = \mathrm{diag}(k_{11}, \ldots, k_{1n}).$$

The next lemma (with derivation given in the App.) supplies a generic condition under which the specific hyperbolic relationship will appear.

Lemma 4.2. If the stationary weights $\mathbf{w}$ in (4.3) do not depend on $[S]$, then the reaction rate v has a hyperbolic dependence on $[S]$:

$$v = \frac{\chi[S]}{[S]+C_M}, \quad (4.4)$$

where the constants

$$\chi = \mathbf{w1}/\{\mathbf{w}(\mathbf{I}-\mathbf{Q}_{CA}^{-1}\mathbf{Q}_{CC})\mathbf{Q}_{BC}^{-1}\mathbf{1}\},$$
$$C_M = \big\{\mathbf{w}(\mathbf{I}-\mathbf{Q}_{CA}^{-1}\mathbf{Q}_{CC})\mathbf{Q}_{BC}^{-1}(\mathbf{Q}_{BA}+\mathbf{Q}_{BC}-\mathbf{Q}_{BB})\tilde{\mathbf{Q}}_{AB}^{-1}\mathbf{1}\big\} / \{\mathbf{w}(\mathbf{I}-\mathbf{Q}_{CA}^{-1}\mathbf{Q}_{CC})\mathbf{Q}_{BC}^{-1}\mathbf{1}\}$$

do not involve $[S]$.

Remark 4. Lemma 4.2 indicates that the hyperbolic expression of $v \propto [S]/([S]+C)$ is not unique to the MM model. Such a formula could readily arise from our model.

Fast Enzyme Reset. In most enzymatic reactions, including those involving β-galactosidase, once the product is released, the enzyme returns very quickly to restart a new cycle (Segel 1993). This biochemical fact is captured in our model (2.4) by letting δ_i $(i = 1, 2, \ldots, n)$, the transition rates from E_i^0 to E_i, go to ∞. For the remainder of this section, we, thus, focus on studying these fast-cycle-reset enzymes.

The reaction rate expression (4.3) in this case can be reduced to

$$v = \{\mathbf{w1}\}/\big\{\mathbf{w}\mathbf{Q}_{BC}^{-1}[\mathbf{I}-(\mathbf{Q}_{BB}-\mathbf{Q}_{BA}-\mathbf{Q}_{BC})\mathbf{Q}_{AB}^{-1}]\mathbf{1}\big\},$$

and (3.11), which determines the weights $\mathbf{w}$, can be simplified to

$$\mathbf{w}(\mathbf{I}+\mathbf{M}\mathbf{Q}_{BC}) = 0; \quad (4.5)$$

the two constants χ and C_M in Lemma 4.2 become

$$\chi = \mathbf{w1}/\{\mathbf{w}\mathbf{Q}_{BC}^{-1}\mathbf{1}\},$$
$$C_M = \{\mathbf{w}\mathbf{Q}_{BC}^{-1}(\mathbf{Q}_{BA}+\mathbf{Q}_{BC}-\mathbf{Q}_{BB})\tilde{\mathbf{Q}}_{AB}^{-1}\mathbf{1}\}/\{\mathbf{w}\mathbf{Q}_{BC}^{-1}\mathbf{1}\}. \quad (4.6)$$

The next theorem, whose proof is deferred to the Appendix, identifies six different scenarios; each scenario guarantees the stationary weights $\mathbf{w}$ not depending on $[S]$ and, hence, the hyperbolic relationship (4.4).

Theorem 4.3. For enzymes with fast cycle reset (i.e., after taking the limit of $\delta_i \to \infty$, $i = 1, \ldots, n$), if any one of the following six scenarios holds, then the stationary weights $\mathbf{w}$ will not depend on the concentration $[S]$, and, hence, the reaction rate will obey

$$v = \frac{\chi[S]}{[S]+C_M}.$$

Scenario 1. There are no or negligible transitions among the E_i states; that is, $\mathbf{Q}_{AA} \to 0$, in which case $\chi = \{\boldsymbol{\phi}_B\mathbf{Q}_{BC}\mathbf{1}\}/\{\boldsymbol{\phi}_B\mathbf{1}\}$ and $C_M = \{\boldsymbol{\phi}_B(\mathbf{Q}_{BA}+\mathbf{Q}_{BC})\tilde{\mathbf{Q}}_{AB}^{-1}\mathbf{1}\}/\{\boldsymbol{\phi}_B\mathbf{1}\}$.

Scenario 2. There are no or negligible transitions among the ES_i states; that is, $\mathbf{Q}_{BB} \to 0$, in which case $\chi = \{\boldsymbol{\phi}_A\tilde{\mathbf{Q}}_{AB} \times (\mathbf{Q}_{BA}+\mathbf{Q}_{BC})^{-1}\mathbf{Q}_{BC}\mathbf{1}\}/\{\boldsymbol{\phi}_A\tilde{\mathbf{Q}}_{AB}(\mathbf{Q}_{BA}+\mathbf{Q}_{BC})^{-1}\mathbf{1}\}$ and $C_M = \{\boldsymbol{\phi}_A\mathbf{1}\}/\{\boldsymbol{\phi}_A\tilde{\mathbf{Q}}_{AB}(\mathbf{Q}_{BA}+\mathbf{Q}_{BC})^{-1}\mathbf{1}\}$.

Scenario 3. The transitions among the E_i states are much faster than the others; that is, $\mathbf{Q}_{AA} = \kappa\tilde{\mathbf{Q}}_{AA}$, and the scale κ is much larger than the other transition rates: $\kappa \to \infty$. In this case $\chi = \{\boldsymbol{\phi}_A\tilde{\mathbf{Q}}_{AB}(\mathbf{Q}_{BB} - \mathbf{Q}_{BA} - \mathbf{Q}_{BC})^{-1}\mathbf{Q}_{BC}\mathbf{1}\}/\{\boldsymbol{\phi}_A\tilde{\mathbf{Q}}_{AB}(\mathbf{Q}_{BB} - \mathbf{Q}_{BA} - \mathbf{Q}_{BC})^{-1}\mathbf{1}\}$ and $C_M = \{\boldsymbol{\phi}_A\mathbf{1}\}/\{\boldsymbol{\phi}_A\tilde{\mathbf{Q}}_{AB}(\mathbf{Q}_{BA} + \mathbf{Q}_{BC} - \mathbf{Q}_{BB})^{-1}\mathbf{1}\}$.

Scenario 4. The transitions among the ES_i states are much faster than the others; that is, $\mathbf{Q}_{BB} = \kappa\tilde{\mathbf{Q}}_{BB}$, and the scale κ is much larger than the other transition rates: $\kappa \to \infty$. In this case $\chi = \{\boldsymbol{\phi}_B\mathbf{Q}_{BC}\mathbf{1}\}/\{\boldsymbol{\phi}_B\mathbf{1}\}$ and $C_M = \{\boldsymbol{\phi}_B(\mathbf{Q}_{BA} + \mathbf{Q}_{BC})\tilde{\mathbf{Q}}_{AB}^{-1}\mathbf{1}\}/\{\boldsymbol{\phi}_B\mathbf{1}\}$.

Scenario 5. The transition rate from ES_i to E_i is much larger than the rate from ES_i to E_i^0; that is, $k_{-1i} \gg k_{2i}$ for $i = 1, 2, \ldots, n$. In this case $\chi = \{\boldsymbol{\phi}_B\mathbf{Q}_{BC}\mathbf{1}\}/\{\boldsymbol{\phi}_B\mathbf{1}\}$ and $C_M = \{\boldsymbol{\phi}_B(\mathbf{Q}_{BA} + \mathbf{Q}_{BC})\tilde{\mathbf{Q}}_{AB}^{-1}\mathbf{1}\}/\{\boldsymbol{\phi}_B\mathbf{1}\}$.

Scenario 6. For all the ES_i states, the ratios between the forward and backward transition rates are the same: $k_{21}/k_{-11} = k_{22}/k_{-12} = \cdots = k_{2i}/k_{-1i} = \cdots = k_{2n}/k_{-1n}$. In this case $\chi = \{\boldsymbol{\phi}_B\mathbf{Q}_{BC}\mathbf{1}\}/\{\boldsymbol{\phi}_B\mathbf{1}\}$ and $C_M = \{\boldsymbol{\phi}_B(\mathbf{Q}_{BA} + \mathbf{Q}_{BC})\tilde{\mathbf{Q}}_{AB}^{-1}\mathbf{1}\}/\{\boldsymbol{\phi}_B\mathbf{1}\}$.

Note that the row vectors $\boldsymbol{\phi}_A$ and $\boldsymbol{\phi}_B$ referred to previously are defined by (3.3) and (3.4).

The six scenarios in Theorem 4.3, each covering a large class of enzymes, have their biochemical implications. Scenarios 1 and 2 correspond to the so-called slow fluctuating enzymes, those whose conformations fluctuate/interconvert slowly; Scenarios 3 and 4 correspond to fast fluctuating enzymes, those having fast conformational fluctuations; Scenario 5 corresponds to the so-called primitive enzymes, those whose dissociation rate is much larger than their catalytic rate (Albery and Knowles 1976; Min et al. 2006); Scenario 6 corresponds to conformational-equilibrium enzymes, those possessing the chemical property that the energy–barrier difference between their dissociation and catalysis is invariant across conformations (Min et al. 2006).

By pointing out various general cases under which the hyperbolic relationship between v and $[S]$ arises from our model, Theorem 4.3 and Lemma 4.2 provide an explanation of the third experimental puzzle: Although the MM model gives the description of $v \propto [S]/([S] + C)$, observing such a relationship in experiments by no means implies that the MM model is the underlying mechanism because the MM model is only one of many that display such a relationship—the discovery of memory and heavier-than-exponential distribution of the turnover times points to the opposite direction. This understanding helps reconcile the long-held belief in the MM model with the recent single-molecule experimental surprises. For decades, numerous traditional experiments on different enzymes yielded the $v \propto [S]/([S] + C)$ relationship; because of this, they were viewed as strong evidence for the MM model. Now we know that these traditional experimental outcomes can be better viewed as evidence for our more general stochastic network model.

5. FROM THEORY TO EXPERIMENTAL DATA

A recent single-molecule experiment (English et al. 2006) conducted by the Xie group at Harvard University (Department of Chemistry and Chemical Biology) studied β-galactosidase (β-gal), an essential enzyme in the human body that catalyzes the breakdown of the sugar lactose (Jacobson et al. 1994; Dorland 2003). In the experiment a single β-gal molecule is immobilized (to a bead), which allows its enzymatic turnovers to be continuously monitored under a fluorescence microscope. To detect the individual turnovers, careful design and special treatment were carried out so that once the experimental system was placed under a laser beam the reaction product and *only* the reaction product was fluorescent. This setting ensures that as the β-gal enzyme catalyzes one substrate molecule after another, a strong fluorescence signal is emitted and detected only when a product is released, that is, only when the enzyme reaches the $E_i^0 + P$ stage [see (2.1) and (2.4) for diagrams]. Recording the fluorescence signals over time thus enables the experimental determination of individual turnovers.

Figure 2(a) presents a schematic picture of the experimental setup. Figure 2(b) shows a typical fluorescence intensity reading from the experiment: Each vertical bar is a fluorescence intensity spike generated by the release of *one* reaction product.

Because β-gal is a fast-reset enzyme (Sec. 4.3), the time lag between two adjacent fluorescence spikes is the enzymatic turnover time. Thus, by moving along the time axis and taking the time lag between every two consecutive fluorescence spikes [the vertical bars in Fig. 2(b)], one obtains the successive turnover times of the β-gal molecule (in this way the raw experimental record was translated into numerical datasets).

To investigate how the substrate concentration $[S]$ affects the turnover times, the experiment was repeated at different levels of $[S]$; throughout each repetition the substrate concentration $[S]$ is held at a fixed level.

5.1 Experimental Turnover Time Distributions

The empirical distributions of the experimental turnover times obtained at four substrate concentrations $[S] = 10\ \mu$M, 20 μM, 50 μM, and 100 μM (micromolar) are plotted in Figure 3 on a log-linear scale (open circles, filled circles, open squares, and filled squares correspond to the four substrate concentrations, respectively). Rather than following straight lines on the logarithmic scale as the MM model predicts, the empirical distributions have curved tails at high substrate concentrations.

Applying Pearson's chi-squared test, we assess the goodness of fit of the MM model. Using 10 equally spaced bins (along the x axis), we calculate the Pearson chi-squared statistic $\sum_i (O_i - E_i)^2/E_i$, where the expected bin counts E_i are calculated from (2.2). For the experimental data at $[S] = 50\ \mu$M and 100 μM, the p values are both less than 1%.

A careful reader might ask: Why were the curved tails not observed in the classical population-based ensemble experiments? The answer is that, although, in principle, the classical experiments should also observe these curved tails, in practice, without the capability to track individual enzymes, the classical experiments can only record the fast reaction turnovers, and the slow turnovers that constitute the curved tails are entirely missing.

Now, as a check of our stochastic network model, we fit it to the empirical turnover time distributions. To do so, we note that the model parameters need to be constrained/simplified because so far there are too many.

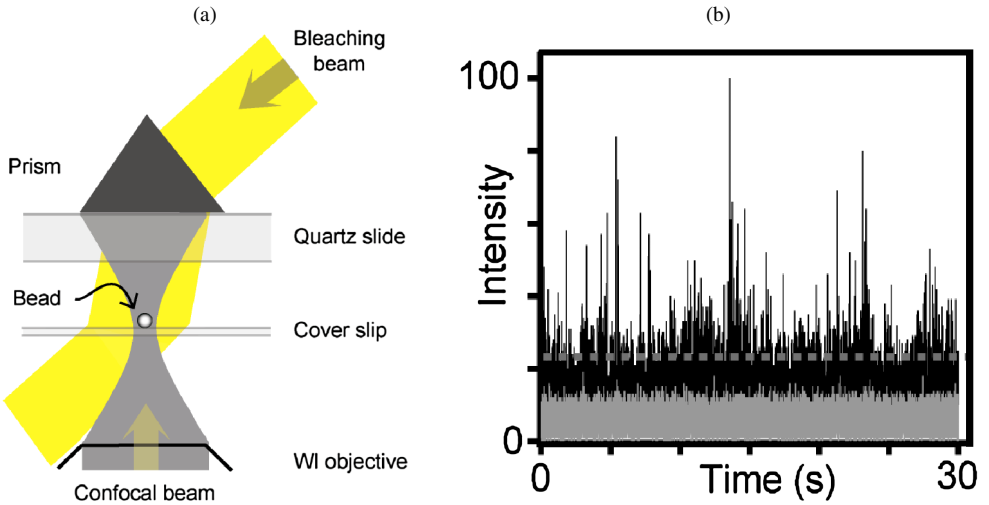

Figure 2. (a) Schematic presentation of the experimental setup. A single β-gal molecule is immobilized to a bead on a glass cover slip. Two laser beams (confocal beam and bleaching beam) are applied to make sure that only the reaction product is fluorescent. By recording the fluorescence signals over time, one can resolve the individual turnovers of the β-gal molecule. (b) Experimental fluorescence intensity reading. Each fluorescence intensity spike is caused by the release of a reaction product.

5.1.1 Parameter Simplification Under the Stochastic Network Model. An important piece of information for simplification comes from Figure 3, which shows that at low substrate concentrations ($[S] = 10\ \mu$M and 20 μM), the empirical distributions are roughly exponential, whereas at high concentrations ($[S] = 50\ \mu$M and 100 μM), the empirical distributions are heavier than exponential. In our model (2.4) at low $[S]$ the transition rates $k_{1i}[S]$ from E_i to ES_i become small compared with the other rates, which implies that at low $[S]$ the slow transitions from E_i to ES_i make up and determine most of the turnover times. The near-exponential empirical distributions at low $[S]$, therefore, point to the homogeneity of the k_{1i}'s (because homogeneous k_{1i} are most consistent with the near-exponential picture). At high $[S]$ the transition rates $k_{1i}[S]$ from E_i to ES_i in our model become large compared with the others, implying that at high $[S]$ the transitions from ES_i to E_i^0 (with rates k_{2i}) will make up and determine most of the turnover times instead. The heavier-than-exponential empirical distributions at high concentrations, hence, point to the heterogeneity of the k_{2i}'s. Incorporating these ideas, we make the first parameter simplification for model fitting: $k_{11} = k_{12} = \cdots = k_{1n} \equiv k_1$, $k_{-11} = k_{-12} = \cdots = k_{-1n} \equiv k_{-1}$, while k_{2i} keep distinct values.

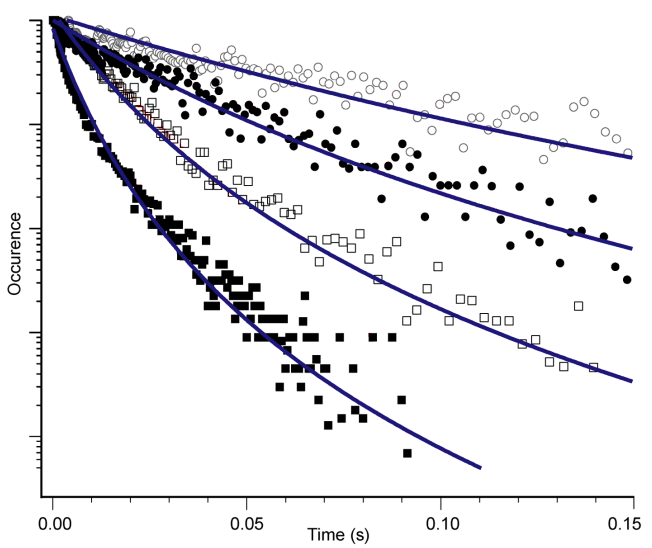

Figure 3. Empirical distributions of the turnover times on a log-linear scale. The open circles, filled circles, open squares, and filled squares represent experimental data obtained at substrate concentrations of 10 μM, 20 μM, 50 μM, and 100 μM, respectively. The solid curves are the fittings from our model using (5.2), where the fitted parameter $\hat{k}_1 = 5.01 \times 10^7\ \text{M}^{-1}\ \text{s}^{-1}$, $\hat{k}_{-1} = 1.83 \times 10^5\ \text{s}^{-1}$, $\hat{a} = 4.25$, and $\hat{b} = 220\ \text{s}^{-1}$.

The second simplification comes from the experimental observation of the hyperbolic relationship between the reaction rate v and $[S]$ (Sec. 5.2). Guided by Theorem 4.3, we invoke Scenarios 1 and 2, that is, the slow-fluctuating condition, because recent single-molecule experiments (Lu et al. 1998; Yang et al. 2003; Min et al. 2005b) suggest slow conformational fluctuation in enzymes and in enzyme–substrate complexes. We, thus, make the second parameter simplification: $Q_{AA} = O(\varepsilon)$, $Q_{BB} = O(\varepsilon^{1+d})$, and $\varepsilon \to 0$, $d > 0$.

Under these two simplifications, the Laplace transform (4.1) of the equilibrium turnover time distribution reduces to (after some algebra)

$$\tilde{f}_{\text{eq}}(s) = \frac{1}{\sum_{i=1}^{n} w_i} \left(\sum_{i=1}^{n} w_i \times \frac{k_1 k_{2i}[S]}{k_1 k_{2i}[S] + s(k_1[S] + k_{2i} + k_{-1}) + s^2} \right), \quad (5.1)$$

where the weights w_i, according to the proof of Theorem 4.3 in the Appendix, are given by $w_i = \phi_{Ai} k_1 k_{2i}/(k_{-1} + k_{2i})$ with $\boldsymbol{\phi}_A$ defined in (3.3).

The total number n of conformation states is unknown, as the individual conformations are not observed in the experiment. But the general consensus is that n is large (because an enzyme can change its three-dimensional shape in a very broad range).

A continuum approximation to (5.1), thus, appears reasonable, leading to

$$\tilde{f}_{\text{eq}}(s) = \int_0^\infty w(k_2) \frac{k_1 k_2[S]}{k_1 k_2[S] + s(k_1[S] + k_2 + k_{-1}) + s^2}\, dk_2,$$

where $w(k_2)$ is the continuum approximation of the weights w_i, expressed in terms of a continuous k_2. The simplest distribution over the positive real line is the gamma distribution. Taking $w(k_2)$ to be a gamma density, we reach the final simplification form for data fitting:

$$\tilde{f}_{\text{eq}}(s) = \int_0^\infty \frac{k_2^{a-1}\exp(-k_2/b)}{b^a\Gamma(a)} \times \frac{k_1 k_2[S]}{k_1 k_2[S] + s(k_1[S] + k_2 + k_{-1}) + s^2}\, dk_2,$$

where a and b are the two parameters of the gamma density. In the time domain the preceding expression translates to

$$\begin{aligned} f_{\text{eq}}(t) &= \int_0^\infty \frac{k_2^{a-1}\exp(-k_2/b)}{b^a\Gamma(a)} \frac{k_1 k_2[S]}{2p(k_2)} \times \left(e^{-[q(k_2)-p(k_2)]t} - e^{-[q(k_2)+p(k_2)]t}\right) dk_2, \\ p(k_2) &= \sqrt{\frac{1}{4}(k_1[S] + k_2 + k_{-1})^2 - k_1 k_2[S]}, \\ q(k_2) &= \frac{1}{2}(k_1[S] + k_2 + k_{-1}). \end{aligned} \tag{5.2}$$

Compared with the initial model, there are only four parameters in (5.2): k_1, k_{-1}, a, and b.

5.1.2 Fitting Our Model to the Data. To fit our simplified turnover time distribution (5.2) to the single-molecule experimental data, we first find the maximum likelihood estimates (MLEs) of the four parameters. Because the gradient of the log-likelihood function $\nabla \log f_{\text{eq}} = \frac{1}{f_{\text{eq}}} \nabla f_{\text{eq}}$, we obtain (after some algebra)

$$\begin{aligned} \frac{\partial f_{\text{eq}}}{\partial k_1} &= \int_0^\infty \frac{k_2^{a-1}\exp(-k_2/b)}{b^a\Gamma(a)} \frac{k_2[S]}{2p} \times \left\{ g - \frac{k_1}{p}\frac{[S]}{2p}(q - k_2)g + k_1 \frac{t[S]}{2}\left\{\frac{q - k_2}{p}h - g\right\}\right\} dk_2, \\ \frac{\partial f_{\text{eq}}}{\partial k_{-1}} &= \int_0^\infty \frac{k_2^{a-1}\exp(-k_2/b)}{b^a\Gamma(a)} \frac{k_1 k_2[S]}{4p^2} \times \left\{ qht - \left(pt + \frac{q}{p}\right)g\right\} dk_2, \\ \frac{\partial f_{\text{eq}}}{\partial a} &= \int_0^\infty \frac{k_2^{a-1}\exp(-k_2/b)}{b^a\Gamma(a)} \left(\log k_2 - \log b - \frac{\Gamma'(a)}{\Gamma(a)}\right) \times \frac{k_1 k_2[S]}{2p} g\, dk_2, \\ \frac{\partial f_{\text{eq}}}{\partial b} &= \int_0^\infty \frac{k_2^{a-1}\exp(-k_2/b)}{\Gamma(a) b^{a+2}} \frac{k_1 k_2[S]}{2p}(k_2 - ab) g\, dk_2, \end{aligned}$$

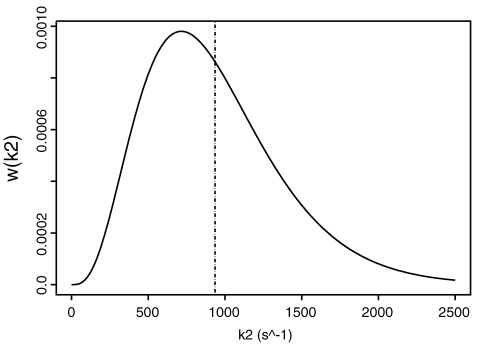

Figure 4. Gamma distribution $w(k_2) = k_2^{a-1}\exp(-k_2/b)/[b^a \times \Gamma(a)]$ of k_2, using the fitted $\hat{a}$ and $\hat{b}$. The dashed vertical line is the mean of the distribution.

where for notational ease p, q, g, and h denote the following:

$$\begin{aligned} p &\triangleq \sqrt{\frac{1}{4}(k_1[S] + k_2 + k_{-1})^2 - k_1 k_2[S]}, \\ q &\triangleq \frac{1}{2}(k_1[S] + k_2 + k_{-1}), \\ g &\triangleq \exp(-(q - p)t) - \exp(-(q + p)t), \\ h &\triangleq \exp(-(q - p)t) + \exp(-(q + p)t). \end{aligned}$$

The integrals in f_{eq} and ∇f_{eq} cannot be evaluated analytically. Hence, we used numerical integration and the conjugate gradient method (the Polak–Ribiere method in particular), which only requires knowledge of first derivatives (see Press, Flannery, Teukolsky, and Vetterling 1992), to find the maximum likelihood estimates, and we obtained $\hat{k}_1 = 5.01 \times 10^7\ \text{M}^{-1}\ \text{s}^{-1}$, $\hat{k}_{-1} = 1.83 \times 10^5\ \text{s}^{-1}$, $\hat{a} = 4.25$, and $\hat{b} = 220\ \text{s}^{-1}$.

Using the MLEs, we fit our turnover time distribution (5.2) to the experimental data, shown in Figure 3 as the solid curves (overlaid on the empirical distributions). For all four substrate concentrations, close agreement between the theoretical curves and the experimental values is evident. Figure 4 plots the gamma distribution $w(k_2) = k_2^{a-1}\exp(-k_2/b)/[b^a\Gamma(a)]$ of k_2, using the fitted $\hat{a}$ and $\hat{b}$. It is clear that the rate k_2 varies over a broad range, which contrasts sharply with the MM assumption of a constant k_2.

5.2 Experimental Relationship Between Reaction Rate and Substrate Concentration

At each substrate concentration $[S]$, the reaction rate can be directly calculated from the experimental turnover times $T_1, T_2, T_3, \ldots, T_N$ via $\hat{v} = 1/\bar{T}$. If the hyperbolic relationship of

$$v = \chi[S]/([S] + C_M)$$

holds, then a plot of $1/v$ versus $1/[S]$ should yield a straight line with slope C_M/χ and intercept $1/\chi$. Figure 5 graphs $1/\hat{v}$ versus $1/[S]$ from experimental data. Notably, a linear pattern indeed emerges. A simple least squares fit (the black line in Fig. 5) gives $\hat{\chi} = 730\ \text{s}^{-1}$ and $\hat{C}_M = 390\ \mu\text{M}$ with standard errors $40\ \text{s}^{-1}$ and $30\ \mu\text{M}$, respectively.

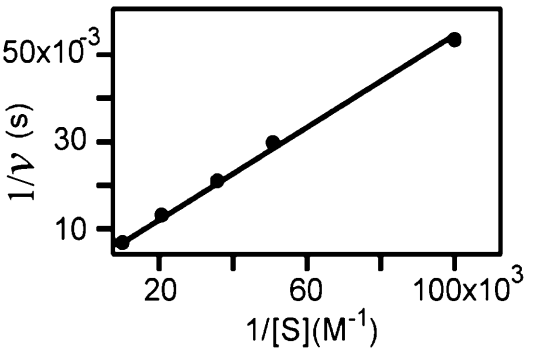

Figure 5. Plot of $1/\hat{v}$ versus $1/[S]$ from the experimental data. The reaction rate $\hat{v}$ at each point is calculated from the experimental data at the corresponding substrate concentration. The black line is the least squares fit with $\hat{\chi} = 730 \pm 80\ \mathrm{s}^{-1}$ and $\hat{C}_M = 390 \pm 60\ \mu\mathrm{M}$.

As a consistency check of our model, we compute from formula (5.2) that

$$\begin{aligned}\mu_{\mathrm{eq}} &= \int_0^\infty t f_{\mathrm{eq}}(t)\,dt \\ &= \int_0^\infty \frac{k_2^{a-1}\exp(-k_2/b)}{b^a\Gamma(a)}\,\frac{k_1[S]+k_2+k_{-1}}{k_1k_2[S]}\,dk_2 \\ &= \frac{[S]+(k_{-1}+b(a-1))/k_1}{b(a-1)[S]},\end{aligned}$$

which gives

$$v = \frac{1}{\mu_{\mathrm{eq}}} = \frac{b(a-1)[S]}{[S]+(k_{-1}+b(a-1))/k_1} \equiv \frac{\chi'[S]}{[S]+C'_M}.$$

Plugging in the MLEs of Figure 3, we note that $\hat{\chi}' = \hat{b}(\hat{a}-1) = 715\ \mathrm{s}^{-1}$ and $\hat{C}'_M = (\hat{k}_{-1} + \hat{b}(\hat{a}-1))/\hat{k}_1 = 380\ \mu\mathrm{M}$ agree well with the least squares *nonparametric* estimates of $\hat{\chi} = 730 \pm 80\ \mathrm{s}^{-1}$ and $\hat{C}_M = 390 \pm 60\ \mu\mathrm{M}$ given previously (mean plus/minus twice the standard error).

5.3 Experimental Autocorrelation of Turnover Times

From the experimental successive turnover times $T_1, T_2, T_3, \ldots, T_N$, one can calculate their empirical autocovariance

$$\mathrm{Cov}(m) = \frac{1}{N-m}\sum_i (T_i - \bar{T})(T_{i+m} - \bar{T}).$$

Figure 6 shows the empirical autocorrelation function, plotting the normalized $\mathrm{Cov}(m)$ against $m\bar{T}$ for $m = 1, 2, \ldots$ at a representative substrate concentration $[S] = 100\ \mu\mathrm{M}$. Instead of a flat horizontal line at 0 as the MM model would predict, a clear memory effect is seen in Figure 6. The experimental data at other substrate concentrations showed a similar correlation picture. The evident memory indicates strongly that the classical MM missed important aspects of real enzymatic reactions and that models like ours that can account for the memory are necessary.

6. DISCUSSION

In this article we introduce a stochastic network model to explain the experimental puzzles arising from single-molecule studies of enzymatic reactions. The use of the multiple states

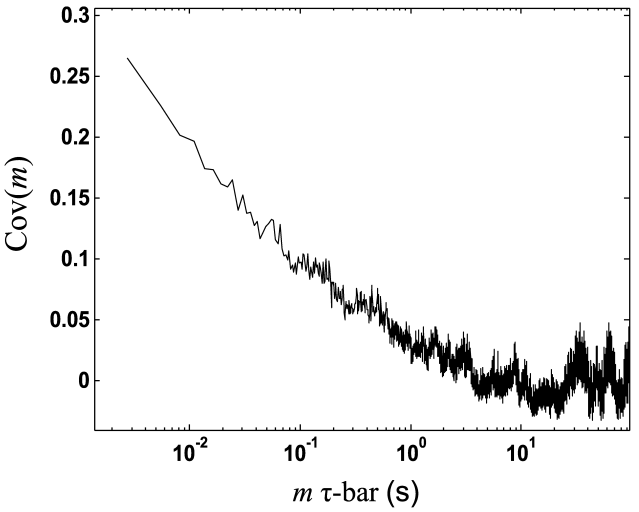

Figure 6. Turnover time autocorrelation function. $\mathrm{Cov}(m)$ is plotted against $m\bar{T}$ from the experimental data at substrate concentration $[S] = 100\ \mu\mathrm{M}$.

(to capture the enzyme's conformational fluctuation) plays a fundamental role in the model's success. We conduct a detailed study of the model (such as analyzing the first-passage-time distributions). Using the analytical results, we show that the model explains (a) the heavier-than-exponential empirical turnover time distributions, (b) the memory effect of turnover times, and (c) the observed hyperbolic relationship between enzymatic reaction rate and substrate concentration.

The model has three additional appealing features. (1) It offers analytical tractability as the results in Sections 3 and 4 illustrate. (2) The theoretical results from the model agree well with the experimental data (as seen in Sec. 5). (3) The model has a solid biological/chemical underpinning—each component and parameter in the model has its biological/chemical meaning.

Some problems remain open for future exploration.

1. When we estimated the model parameters in Section 5.1, we first calculated the log-likelihood by adding up the log-density contribution from each observed turnover time and then maximized it. Because this calculation essentially ignores the correlation of the turnover times, it is, in fact, a quasi-likelihood method (Heyde 1997). Although ergodicity ensures the consistency, a theoretical investigation of its efficiency remains open.
2. We simultaneously fit the turnover time distributions at multiple concentrations. Extending the fitting to the autocorrelation functions is open for further study.
3. When we fit our model to the experimental data, we used the continuum limit by letting the number of states n go to ∞ and then assumed a gamma distribution. Although this simple approach fits the experimental data well, it remains to be seen if the continuum limit and gamma distribution can be derived directly from a more biological/biophysical microscopic angle. Such study will provide an interesting connection between statistics and biophysics by giving the statistical assumptions a biological underpinning; it will, furthermore, lead to not only potentially better approximation schemes, but also new insight into the biological nature of an enzyme's conformation

fluctuation (e.g., the potential mean field in the conformation space).

4. In fitting the data we applied the slow-fluctuating-enzyme condition, because it appeared most natural. A problem for future study is to explore the other scenarios of Theorem 4.3, investigate how to constrain the model parameters under these scenarios, and compare their fittings to the data. Such investigation will help pin down the role that conformational fluctuation plays in enzymatic reactions and can potentially guide the design of new experiments to elucidate the underlying microscopic biophysical picture.

The new field of nanoscale (single-molecule) biophysics has attracted much attention from biologists, chemists, and physicists, as it holds promise for new scientific discoveries. It also presents many interesting problems for statisticians because of the stochastic nature of the nanometer world. Our stochastic network model for single-molecule enzymatic reaction exemplifies only one instance of the numerous and growing research opportunities in nanoscale biophysics. We hope that this article will generate further interest in applying modern statistical and probabilistic methodology to interesting biophysical and scientific problems.

APPENDIX: PROOFS

Proof of Proposition 2.1

To obtain the turnover time distribution under the MM model, let T_E and T_{ES} denote the first passage times to reach E^0 from states E and ES, respectively, and let $f_E(t)$ and $f_{ES}(t)$ be their corresponding density functions. The routing map (2.1) immediately gives

$$T_E \stackrel{d}{=} \mathcal{E}_{k_1[S]} + T_{ES}, \tag{A.1}$$

where the random variables on the right side are independent of each other, and throughout this proof, $\mathcal{E}_\rho$ denotes an exponential random variable with rate ρ. Next, noting that one can go either forward or backward from state ES with the two directions characterized by two exponential random variables $\mathcal{E}_{k_2}$ and $\mathcal{E}_{k_{-1}}$, we have

$$\begin{aligned}
f_{ES}(t)\,dt &= P(T_{ES} \in (t, t+dt)) \\
&= P\bigl(T_{ES} \in (t, t+dt), \mathcal{E}_{k_2} < \mathcal{E}_{k_{-1}}\bigr) \\
&\quad + P\bigl(T_{ES} \in (t, t+dt), \mathcal{E}_{k_2} > \mathcal{E}_{k_{-1}}\bigr) \\
&= P\bigl(\mathcal{E}_{k_2} \in (t, t+dt), \mathcal{E}_{k_2} < \mathcal{E}_{k_{-1}}\bigr) \\
&\quad + P\bigl(\mathcal{E}_{k_{-1}} + T_E \in (t, t+dt), \mathcal{E}_{k_2} > \mathcal{E}_{k_{-1}}\bigr) \\
&= k_2 e^{-(k_2+k_{-1})t}\,dt \\
&\quad + \left(\int_0^t f_E(t-z) k_{-1} e^{-(k_2+k_{-1})z}\,dz\right) dt \\
&\quad + o(dt).
\end{aligned} \tag{A.2}$$

In the Laplace space (A.1) and (A.2) become

$$\tilde{f}_E(s) = \frac{k_1[S]}{k_1[S]+s}\tilde{f}_{ES}(s),$$

$$\tilde{f}_{ES}(s) = \frac{k_2}{k_2+k_{-1}+s} + \frac{k_{-1}}{k_2+k_{-1}+s}\tilde{f}_E(s),$$

where $\tilde{f}_E(s)$ and $\tilde{f}_{ES}(s)$ are the Laplace transforms of $f_E(t)$ and $f_{ES}(t)$, respectively [i.e., $\tilde{f}_J(s) = \int_0^\infty e^{-st} f_J(t)\,dt$, $J = E$ or ES]. Solving them, we obtain

$$\tilde{f}_E(s) = \frac{k_1 k_2 [S]}{k_1 k_2 [S] + s(k_1[S] + k_2 + k_{-1}) + s^2},$$

and correspondingly the density function of the turnover time is

$$f_E(t) = k_1 k_2 [S]\bigl(e^{-(q-p)t} - e^{-(q+p)t}\bigr)/(2p),$$

where $p = \sqrt{(k_1[S]+k_2+k_{-1})^2/4 - k_1 k_2 [S]}$ and $q = (k_1[S]+k_2+k_{-1})/2$.

Proof of Lemma 3.1

Let Y_n denote the embedded Markov chain associated with $X(t)$ [i.e., Y_n is the discrete-time Markov chain corresponding to the jumps of $X(t)$]. It is straightforward to check that Y_n is irreducible and aperiodic and is, thus, positive recurrent. This guarantees that (see Kijima 1997) (1) $X(t)$ is ergodic, (2) the stationary distribution of $X(t)$ exists and is unique, and (3) the stationary distribution satisfies $(\boldsymbol{\pi}_A, \boldsymbol{\pi}_B, \boldsymbol{\pi}_C)\mathbf{Q} = 0$. The definition (2.5) of $\mathbf{Q}$ then gives

$$\begin{aligned}
&(\boldsymbol{\pi}_A, \boldsymbol{\pi}_B, \boldsymbol{\pi}_C) \\
&\quad \times \begin{pmatrix} \mathbf{Q}_{AA} - \mathbf{Q}_{AB} & \mathbf{Q}_{AB} & \mathbf{0} \\ \mathbf{Q}_{BA} & \mathbf{Q}_{BB} - (\mathbf{Q}_{BA} + \mathbf{Q}_{BC}) & \mathbf{Q}_{BC} \\ \mathbf{Q}_{CA} & \mathbf{0} & \mathbf{Q}_{CC} - \mathbf{Q}_{CA} \end{pmatrix} = 0,
\end{aligned}$$

which implies that

$$\begin{aligned}
&(\boldsymbol{\pi}_A, \boldsymbol{\pi}_B) \begin{pmatrix} \mathbf{Q}_{AA} - \mathbf{Q}_{AB} & \mathbf{Q}_{AB} \\ \mathbf{Q}_{BA} & \mathbf{Q}_{BB} - (\mathbf{Q}_{BA} + \mathbf{Q}_{BC}) \end{pmatrix} \\
&\quad + \boldsymbol{\pi}_C \begin{pmatrix} \mathbf{Q}_{CA} & \mathbf{0} \end{pmatrix} = 0,
\end{aligned} \tag{A.3}$$

$$\boldsymbol{\pi}_B \mathbf{Q}_{BC} + \boldsymbol{\pi}_C (\mathbf{Q}_{CC} - \mathbf{Q}_{CA}) = 0. \tag{A.4}$$

From (A.3) we have

$$\begin{aligned}
(\boldsymbol{\pi}_A, \boldsymbol{\pi}_B) &= -\boldsymbol{\pi}_C \begin{pmatrix} \mathbf{Q}_{CA} & \mathbf{0} \end{pmatrix} \\
&\quad \times \begin{pmatrix} \mathbf{Q}_{AA} - \mathbf{Q}_{AB} & \mathbf{Q}_{AB} \\ \mathbf{Q}_{BA} & \mathbf{Q}_{BB} - (\mathbf{Q}_{BA} + \mathbf{Q}_{BC}) \end{pmatrix}^{-1}.
\end{aligned}$$

The formula for block-matrix inversion provides

$$\begin{pmatrix} \mathbf{Q}_{AA} - \mathbf{Q}_{AB} & \mathbf{Q}_{AB} \\ \mathbf{Q}_{BA} & \mathbf{Q}_{BB} - (\mathbf{Q}_{BA} + \mathbf{Q}_{BC}) \end{pmatrix}^{-1} = \begin{pmatrix} \mathbf{L} & \mathbf{M} \\ \mathbf{N} & \mathbf{R} \end{pmatrix}, \tag{A.5}$$

where

$$\begin{aligned}
\mathbf{L} &= [\mathbf{Q}_{AA} - \mathbf{Q}_{AB} - \mathbf{Q}_{AB}(\mathbf{Q}_{BB} - \mathbf{Q}_{BA} - \mathbf{Q}_{BC})^{-1}\mathbf{Q}_{BA}]^{-1}, \\
\mathbf{M} &= [\mathbf{Q}_{BB} - \mathbf{Q}_{BC} - (\mathbf{Q}_{BB} - \mathbf{Q}_{BA} - \mathbf{Q}_{BC})\mathbf{Q}_{AB}^{-1}\mathbf{Q}_{AA}]^{-1}, \\
\mathbf{N} &= [\mathbf{Q}_{AA} - (\mathbf{Q}_{AA} - \mathbf{Q}_{AB})\mathbf{Q}_{BA}^{-1}(\mathbf{Q}_{BB} - \mathbf{Q}_{BC})]^{-1}, \\
\mathbf{R} &= [\mathbf{Q}_{BB} - \mathbf{Q}_{BA} - \mathbf{Q}_{BC} - \mathbf{Q}_{BA}(\mathbf{Q}_{AA} - \mathbf{Q}_{AB})^{-1}\mathbf{Q}_{AB}]^{-1}.
\end{aligned} \tag{A.6}$$

Therefore,

$$\begin{aligned}
(\boldsymbol{\pi}_A, \boldsymbol{\pi}_B) &= -\boldsymbol{\pi}_C \begin{pmatrix} \mathbf{Q}_{CA} & \mathbf{0} \end{pmatrix} \begin{pmatrix} \mathbf{L} & \mathbf{M} \\ \mathbf{N} & \mathbf{R} \end{pmatrix} \\
&= -(\boldsymbol{\pi}_C \mathbf{Q}_{CA} \mathbf{L},\ \boldsymbol{\pi}_C \mathbf{Q}_{CA} \mathbf{M}),
\end{aligned} \tag{A.7}$$

Substituting (A.7) into (A.4), we have the final equation for $\boldsymbol{\pi}_C$: $\boldsymbol{\pi}_C(\mathbf{Q}_{CC} - \mathbf{Q}_{CA} - \mathbf{Q}_{CA}\mathbf{M}\mathbf{Q}_{BC}) = 0$.

Proof of Theorem 3.2

Consider a Markov chain $Z(t)$ modified from $X(t)$ by making $\{E_1^0, \ldots, E_n^0\}$ absorbing (see Keilson 1979; Kijima 1997). It has transition matrix

$$\mathbf{Q}_z = \begin{pmatrix} \mathbf{Q}_{AA} - \mathbf{Q}_{AB} & \mathbf{Q}_{AB} & \mathbf{0} \\ \mathbf{Q}_{BA} & \mathbf{Q}_{BB} - (\mathbf{Q}_{BA} + \mathbf{Q}_{BC}) & \mathbf{Q}_{BC} \\ \mathbf{0} & \mathbf{0} & \mathbf{0} \end{pmatrix}.$$

The first passage time to $\{E_1^0, \ldots, E_n^0\}$ for $X(t)$ is the same as the absorbing time of $Z(t)$. Applying a first-step analysis and noting there is no direct transition from E_i to E_j^0, we have

$$P(T_I \in (t, t+dt)) = \sum_{J \in \{ES_1, \ldots, ES_n\}} \sum_{K \in \{E_1^0, \ldots, E_n^0\}} P_{IJ}(t)(\mathbf{Q}_z)_{JK}\, dt + o(dt) \quad \text{for } I = E_i \text{ or } ES_i,$$

where $P_{IJ}(t)$ is $Z(t)$'s transition probability from state I to state J at time t; in matrix form the equation can be written as

$$\begin{pmatrix} \mathbf{f}_A(t) \\ \mathbf{f}_B(t) \end{pmatrix} dt = \mathbf{P}(t) \begin{pmatrix} \mathbf{0} \\ \mathbf{Q}_{BC}\mathbf{1} \end{pmatrix} dt + o(dt), \tag{A.8}$$

where $\mathbf{P}(t)$ is the sub–transition matrix of $Z(t)$ corresponding to the nonabsorbing states.

The full transition matrix of $Z(t)$ is $\exp(\mathbf{Q}_z t)$, of which $\mathbf{P}(t)$ is the upper-left block. It is straightforward to verify from block-matrix calculation that

$$\mathbf{P}(t) = \exp\left(\begin{pmatrix} \mathbf{Q}_{AA} - \mathbf{Q}_{AB} & \mathbf{Q}_{AB} \\ \mathbf{Q}_{BA} & \mathbf{Q}_{BB} - (\mathbf{Q}_{BA} + \mathbf{Q}_{BC}) \end{pmatrix} t \right),$$

which (according to the basic properties of matrix exponential) has Laplace transform

$$\tilde{\mathbf{P}}(s) = \int_0^\infty \exp(-st)\mathbf{P}(t)\, dt = \left[s\mathbf{I} - \begin{pmatrix} \mathbf{Q}_{AA} - \mathbf{Q}_{AB} & \mathbf{Q}_{AB} \\ \mathbf{Q}_{BA} & \mathbf{Q}_{BB} - \mathbf{Q}_{BA} - \mathbf{Q}_{BC} \end{pmatrix} \right]^{-1}.$$

Applying a Laplace transform on (A.8) and using the previous formula for $\tilde{\mathbf{P}}(s)$, we finally obtain (3.9).

Proof of Corollary 3.3

Equation (3.9) gives

$$s \begin{pmatrix} \tilde{\mathbf{f}}_A(s) \\ \tilde{\mathbf{f}}_B(s) \end{pmatrix} = \begin{pmatrix} \mathbf{Q}_{AA} - \mathbf{Q}_{AB} & \mathbf{Q}_{AB} \\ \mathbf{Q}_{BA} & \mathbf{Q}_{BB} - (\mathbf{Q}_{BA} + \mathbf{Q}_{BC}) \end{pmatrix} \begin{pmatrix} \tilde{\mathbf{f}}_A(s) \\ \tilde{\mathbf{f}}_B(s) \end{pmatrix} + \begin{pmatrix} \mathbf{0} \\ \mathbf{Q}_{BC}\mathbf{1} \end{pmatrix}.$$

Taking the derivative with respect to s in the preceding expression and evaluating it at $s = 0$ yield

$$\begin{pmatrix} \boldsymbol{\mu}_A \\ \boldsymbol{\mu}_B \end{pmatrix} = -\begin{pmatrix} \tilde{\mathbf{f}}'_A(0) \\ \tilde{\mathbf{f}}'_B(0) \end{pmatrix} = -\begin{pmatrix} \mathbf{Q}_{AA} - \mathbf{Q}_{AB} & \mathbf{Q}_{AB} \\ \mathbf{Q}_{BA} & \mathbf{Q}_{BB} - (\mathbf{Q}_{BA} + \mathbf{Q}_{BC}) \end{pmatrix}^{-1} \begin{pmatrix} \mathbf{1} \\ \mathbf{1} \end{pmatrix},$$

which is simplified to (3.10) by the block-matrix inversion (A.5) and (A.6).

Proof of Lemma 3.4

Because a turnover event begins right after the enzyme enters the E_i $(i = 1, 2, \ldots, n)$ state from the E_i^0 state (see Sec. 2.2), it follows that the stationary probability $w(E_i)$ is proportional to the probability flux from E_i^0 to E_i, that is, the expected number of transitions from E_i^0 to E_i per unit time. The latter is given by $\pi(E_i^0)\delta_i$ according to Levy's formula (see Serfozo 1999). Therefore, the weight vector $(w(E_i), \ldots, w(E_n)) \propto \mathbf{w} = \boldsymbol{\pi}_C \mathbf{Q}_{CA}$. According to Lemma 3.1, $\boldsymbol{\pi}_C$ satisfies (3.6), which implies immediately that $\mathbf{w}$ must satisfy (3.11).

Proof of Corollary 3.5

From Lemma 3.4 we know $\mu_{\text{eq}} = (\mathbf{w}\boldsymbol{\mu}_A)/(\mathbf{w}\mathbf{1})$, which by Corollary 3.3 is $\mu_{\text{eq}} = -[\mathbf{w}(\mathbf{L} + \mathbf{M})\mathbf{1}]/(\mathbf{w}\mathbf{1})$. Next, it is straightforward to verify from the definition of $\mathbf{L}$ and $\mathbf{M}$ in Lemma 3.1 that $\mathbf{L} = -\mathbf{M}(\mathbf{Q}_{BB} - \mathbf{Q}_{BA} - \mathbf{Q}_{BC})\mathbf{Q}_{AB}^{-1}$, which implies $\mathbf{L} + \mathbf{M} = -\mathbf{M}[(\mathbf{Q}_{BB} - \mathbf{Q}_{BA} - \mathbf{Q}_{BC})\mathbf{Q}_{AB}^{-1} - \mathbf{I}]$. It, thus, follows that

$$\mu_{\text{eq}} = \frac{1}{\mathbf{w}\mathbf{1}} \mathbf{w}\mathbf{M}[(\mathbf{Q}_{BB} - \mathbf{Q}_{BA} - \mathbf{Q}_{BC})\mathbf{Q}_{AB}^{-1} - \mathbf{I}]\mathbf{1}.$$

The definition (3.11) of $\mathbf{w}$ tells us that $\mathbf{w}\mathbf{M} = \mathbf{w}(\mathbf{Q}_{CA}^{-1}\mathbf{Q}_{CC} - \mathbf{I})\mathbf{Q}_{BC}^{-1}$. Plugging it into the preceding expression yields (3.12).

Proof of Lemma 4.1

The detailed balance condition (3.2) tells us that $\begin{pmatrix} \boldsymbol{\Phi}_A & \mathbf{0} \\ \mathbf{0} & \boldsymbol{\Phi}_B \end{pmatrix}\mathbf{G}$ is symmetric, because $\boldsymbol{\Phi}_A$, $\boldsymbol{\Phi}_B$, $\mathbf{Q}_{AB}$, $\mathbf{Q}_{BA}$, and $\mathbf{Q}_{BC}$ are all diagonal matrices. Hence, the matrix $\begin{pmatrix} \boldsymbol{\Phi}_A & \mathbf{0} \\ \mathbf{0} & \boldsymbol{\Phi}_B \end{pmatrix}^{1/2} \mathbf{G} \begin{pmatrix} \boldsymbol{\Phi}_A & \mathbf{0} \\ \mathbf{0} & \boldsymbol{\Phi}_B \end{pmatrix}^{-1/2}$ is also symmetric and, thus, admits a spectral decomposition. Consequently, $\mathbf{G}$ is diagonalizable: $\mathbf{G} = \mathbf{U}\boldsymbol{\Lambda}\mathbf{U}^{-1} = \sum_{i=1}^{2n} \lambda_i \boldsymbol{\xi}_i \boldsymbol{\eta}_i^T$, where λ_i are the eigenvalues of $\mathbf{G}$, and $\boldsymbol{\xi}_i$ and $\boldsymbol{\eta}_i^T$ are the corresponding right and left eigenvectors, respectively. This implies that

$$(s\mathbf{I} - \mathbf{G})^{-1} = \sum_{i=1}^{2n} \frac{1}{s - \lambda_i} \boldsymbol{\xi}_i \boldsymbol{\eta}_i^T,$$

which means that $\tilde{f}_{\text{eq}}(s)$ can be re-expressed as

$$\tilde{f}_{\text{eq}}(s) = \sum_{i=1}^{2n} \frac{1}{s - \lambda_i} \left[\frac{(\mathbf{w}\ \mathbf{0})\boldsymbol{\xi}_i}{\mathbf{w}\mathbf{1}} \boldsymbol{\eta}_i^T \begin{pmatrix} \mathbf{0} \\ \mathbf{Q}_{BC}\mathbf{1} \end{pmatrix} \right].$$

The matrix $\mathbf{G}$ satisfies

$$\mathbf{G}\mathbf{1} = \begin{pmatrix} \mathbf{Q}_{AA} - \mathbf{Q}_{AB} & \mathbf{Q}_{AB} \\ \mathbf{Q}_{BA} & \mathbf{Q}_{BB} - \mathbf{Q}_{BA} - \mathbf{Q}_{BC} \end{pmatrix} \begin{pmatrix} \mathbf{1} \\ \mathbf{1} \end{pmatrix} = -\begin{pmatrix} \mathbf{0} \\ \mathbf{Q}_{BC}\mathbf{1} \end{pmatrix}. \tag{A.9}$$

Because the diagonal elements of $\mathbf{Q}_{BC}$ are all positive, (A.9) implies that $\mathbf{G}$ is a lossy generator (see Keilson 1979; Kijima 1997), and, hence, all its eigenvalues λ_i are strictly negative. Thus, we can rewrite

$$\tilde{f}_{\text{eq}}(s) = \sum_{i=1}^{2n} \sigma_i \frac{-\lambda_i}{s - \lambda_i}, \qquad \sigma_i = \frac{1}{-\lambda_i} \left[\frac{(\mathbf{w}\ \mathbf{0})\boldsymbol{\xi}_i}{\mathbf{w}\mathbf{1}} \boldsymbol{\eta}_i^T \begin{pmatrix} \mathbf{0} \\ \mathbf{Q}_{BC}\mathbf{1} \end{pmatrix} \right],$$

which translates to $f_{\text{eq}}(t) = \sum_{i=1}^{2n} \sigma_i(-\lambda_i e^{\lambda_i t})$.

Proof of Lemma 4.2

With $\mathbf{w}$ not depending on $[S]$, direct calculation from (4.3) yields

$$\begin{aligned} v &= \{\mathbf{w}\mathbf{1}\} \Big/ \left\{ \mathbf{w}(\mathbf{I} - \mathbf{Q}_{CA}^{-1}\mathbf{Q}_{CC})\mathbf{Q}_{BC}^{-1} \right. \\ &\quad \left. \times \left\{ \mathbf{I} - \frac{1}{[S]}(\mathbf{Q}_{BB} - \mathbf{Q}_{BA} - \mathbf{Q}_{BC})\tilde{\mathbf{Q}}_{AB}^{-1} \right\} \mathbf{1} \right\} \\ &= \big(\mathbf{w}\mathbf{1}/\{\mathbf{w}(\mathbf{I} - \mathbf{Q}_{CA}^{-1}\mathbf{Q}_{CC})\mathbf{Q}_{BC}^{-1}\mathbf{1}\}[S]\big) \\ &\quad \Big/\big([S] - \{\mathbf{w}(\mathbf{I} - \mathbf{Q}_{CA}^{-1}\mathbf{Q}_{CC})\mathbf{Q}_{BC}^{-1}(\mathbf{Q}_{BB} - \mathbf{Q}_{BA} - \mathbf{Q}_{BC})\tilde{\mathbf{Q}}_{AB}^{-1}\mathbf{1}\} \\ &\quad /\{\mathbf{w}(\mathbf{I} - \mathbf{Q}_{CA}^{-1}\mathbf{Q}_{CC})\mathbf{Q}_{BC}^{-1}\mathbf{1}\}\big), \end{aligned}$$

which is (4.4).

Proof of Theorem 4.3

We have seen that for enzymes with fast cycle reset the equilibrium weights $\mathbf{w}$ are determined by (4.5), which is equivalent to $\mathbf{w}(\mathbf{I} + \mathbf{Q}_{BC}^{-1}\mathbf{M}^{-1}) = 0$.

The definition (3.8) of $\mathbf{M}$ gives

$$\begin{aligned} &\mathbf{I} + \mathbf{Q}_{BC}^{-1}\mathbf{M}^{-1} \\ &\quad = \mathbf{Q}_{BC}^{-1}\mathbf{Q}_{BB} - \mathbf{Q}_{BC}^{-1}(\mathbf{Q}_{BB} - \mathbf{Q}_{BA} - \mathbf{Q}_{BC})\mathbf{Q}_{AB}^{-1}\mathbf{Q}_{AA} \\ &\quad = \mathbf{Q}_{BC}^{-1}\mathbf{Q}_{BB} - \mathbf{Q}_{BC}^{-1}(\mathbf{Q}_{BB} - \mathbf{Q}_{BA} - \mathbf{Q}_{BC})\tilde{\mathbf{Q}}_{AB}^{-1}\mathbf{Q}_{AA}/[S]. \end{aligned}$$

Consider Scenario 1 now. This scenario ($\mathbf{Q}_{AA} \to 0$) implies that $\mathbf{I} + \mathbf{Q}_{BC}^{-1}\mathbf{M}^{-1} \to \mathbf{Q}_{BC}^{-1}\mathbf{Q}_{BB}$. So in this case $\mathbf{w}$ is the nonzero solution of $\mathbf{w}\mathbf{Q}_{BC}^{-1}\mathbf{Q}_{BB} = 0$. We know from Section 3.1 that $\boldsymbol{\phi}_B\mathbf{Q}_{BB} = 0$. Therefore, $\mathbf{w} = \boldsymbol{\phi}_B\mathbf{Q}_{BC}$, which does not depend on $[S]$. According to Lemma 4.2 and (4.6), we then have $v = \chi[S]/([S] + C_M)$, where $\chi = \boldsymbol{\phi}_B\mathbf{Q}_{BC}\mathbf{1}/\{\boldsymbol{\phi}_B\mathbf{1}\}$ and $C_M = \{\boldsymbol{\phi}_B(\mathbf{Q}_{BA} + \mathbf{Q}_{BC})\tilde{\mathbf{Q}}_{AB}^{-1}\mathbf{1}\}/\{\boldsymbol{\phi}_B\mathbf{1}\}$.

Consider Scenario 2 next. This scenario ($\mathbf{Q}_{BB} \to 0$) implies that $\mathbf{I} + \mathbf{Q}_{BC}^{-1}\mathbf{M}^{-1} \to \mathbf{Q}_{BC}^{-1}(\mathbf{Q}_{BA} + \mathbf{Q}_{BC})\tilde{\mathbf{Q}}_{AB}^{-1}\mathbf{Q}_{AA}/[S]$. So $\mathbf{w}$ is the solution of $\mathbf{w}\mathbf{Q}_{BC}^{-1}(\mathbf{Q}_{BA} + \mathbf{Q}_{BC})\tilde{\mathbf{Q}}_{AB}^{-1}\mathbf{Q}_{AA} = 0$. We know that $\boldsymbol{\phi}_A\mathbf{Q}_{AA} = 0$ from Section 3.1. Therefore, $\mathbf{w} = \boldsymbol{\phi}_A\tilde{\mathbf{Q}}_{AB}(\mathbf{Q}_{BA} + \mathbf{Q}_{BC})^{-1}\mathbf{Q}_{BC}$, which does not depend on $[S]$. Lemma 4.2 and (4.6) then tell us that $v = \chi[S]/([S] + C_M)$, where $\chi = \{\boldsymbol{\phi}_A\tilde{\mathbf{Q}}_{AB}(\mathbf{Q}_{BA} + \mathbf{Q}_{BC})^{-1}\mathbf{Q}_{BC}\mathbf{1}\}/\{\boldsymbol{\phi}_A\tilde{\mathbf{Q}}_{AB}(\mathbf{Q}_{BA} + \mathbf{Q}_{BC})^{-1}\mathbf{1}\}$ and $C_M = \{\boldsymbol{\phi}_A\mathbf{1}\}/\{\boldsymbol{\phi}_A\tilde{\mathbf{Q}}_{AB}(\mathbf{Q}_{BA} + \mathbf{Q}_{BC})^{-1}\mathbf{1}\}$.

Consider Scenario 3. Under this scenario ($\mathbf{Q}_{AA} = \kappa\tilde{\mathbf{Q}}_{AA}$ with the scale $\kappa \to \infty$), $(\mathbf{I} + \mathbf{Q}_{BC}^{-1}\mathbf{M}^{-1})/\kappa \to -\mathbf{Q}_{BC}^{-1}(\mathbf{Q}_{BB} - \mathbf{Q}_{BA} - \mathbf{Q}_{BC})\tilde{\mathbf{Q}}_{AB}^{-1}\tilde{\mathbf{Q}}_{AA}/[S]$. Hence, $\mathbf{w}$ is the solution of $\mathbf{w}\mathbf{Q}_{BC}^{-1}(\mathbf{Q}_{BB} - \mathbf{Q}_{BA} - \mathbf{Q}_{BC})\tilde{\mathbf{Q}}_{AB}^{-1}\tilde{\mathbf{Q}}_{AA} = 0$. Because $\boldsymbol{\phi}_A\tilde{\mathbf{Q}}_{AA} = 0$, it follows that $\mathbf{w} = \boldsymbol{\phi}_A\tilde{\mathbf{Q}}_{AB}(\mathbf{Q}_{BB} - \mathbf{Q}_{BA} - \mathbf{Q}_{BC})^{-1}\mathbf{Q}_{BC}$, which does not depend on $[S]$. Lemma 4.2 and (4.6) then imply $v = \chi[S]/([S] + C_M)$, where $\chi = \{\boldsymbol{\phi}_A\tilde{\mathbf{Q}}_{AB}(\mathbf{Q}_{BB} - \mathbf{Q}_{BA} - \mathbf{Q}_{BC})^{-1}\mathbf{Q}_{BC}\mathbf{1}\}/\{\boldsymbol{\phi}_A\tilde{\mathbf{Q}}_{AB}(\mathbf{Q}_{BB} - \mathbf{Q}_{BA} - \mathbf{Q}_{BC})^{-1}\mathbf{1}\}$ and $C_M = -\{\boldsymbol{\phi}_A\mathbf{1}\}/\{\boldsymbol{\phi}_A\tilde{\mathbf{Q}}_{AB}(\mathbf{Q}_{BB} - \mathbf{Q}_{BA} - \mathbf{Q}_{BC})^{-1}\mathbf{1}\}$.

Consider Scenario 4. Under this scenario ($\mathbf{Q}_{BB} = \kappa\tilde{\mathbf{Q}}_{BB}$ with the scale $\kappa \to \infty$), $(\mathbf{I} + \mathbf{Q}_{BC}^{-1}\mathbf{M}^{-1})/\kappa \to \mathbf{Q}_{BC}^{-1}\tilde{\mathbf{Q}}_{BB} - \mathbf{Q}_{BC}^{-1}\tilde{\mathbf{Q}}_{BB}\tilde{\mathbf{Q}}_{AB}^{-1} \times \mathbf{Q}_{AA}/[S]$, which tells us that $\mathbf{w}$ is the solution of $\mathbf{w}(\mathbf{Q}_{BC}^{-1}\tilde{\mathbf{Q}}_{BB} - \mathbf{Q}_{BC}^{-1}\tilde{\mathbf{Q}}_{BB}\tilde{\mathbf{Q}}_{AB}^{-1}\mathbf{Q}_{AA}/[S]) = 0$. Because $\boldsymbol{\phi}_B\tilde{\mathbf{Q}}_{BB} = 0$, it follows that $\mathbf{w} = \boldsymbol{\phi}_B\mathbf{Q}_{BC}$, which does not depend on $[S]$. Lemma 4.2 and (4.6) then imply $v = \chi[S]/([S] + C_M)$, where $\chi = \boldsymbol{\phi}_B\mathbf{Q}_{BC}\mathbf{1}/\{\boldsymbol{\phi}_B\mathbf{1}\}$ and $C_M = -\{\boldsymbol{\phi}_B(\mathbf{Q}_{BB} - \mathbf{Q}_{BA} - \mathbf{Q}_{BC})\tilde{\mathbf{Q}}_{AB}^{-1}\mathbf{1}\}/\{\boldsymbol{\phi}_B\mathbf{1}\} = \{\boldsymbol{\phi}_B(\mathbf{Q}_{BA} + \mathbf{Q}_{BC})\tilde{\mathbf{Q}}_{AB}^{-1}\mathbf{1}\}/\{\boldsymbol{\phi}_B\mathbf{1}\}$.

Consider Scenario 5. This scenario ($k_{-1i} \gg k_{2i}$) implies that $\mathbf{Q}_{BA} + \mathbf{Q}_{BC} \approx \mathbf{Q}_{BA}$, so $\mathbf{I} + \mathbf{Q}_{BC}^{-1}\mathbf{M}^{-1} \to \mathbf{Q}_{BC}^{-1}\mathbf{Q}_{BB} - \mathbf{Q}_{BC}^{-1}(\mathbf{Q}_{BB} - \mathbf{Q}_{BA})\tilde{\mathbf{Q}}_{AB}^{-1}\mathbf{Q}_{AA}/[S]$. Therefore, $\mathbf{w}$ is the solution of $\mathbf{w}\{\mathbf{Q}_{BC}^{-1}\mathbf{Q}_{BB} - \mathbf{Q}_{BC}^{-1}(\mathbf{Q}_{BB} - \mathbf{Q}_{BA})\tilde{\mathbf{Q}}_{AB}^{-1}\mathbf{Q}_{AA}/[S]\} = 0$. Using the facts that $\boldsymbol{\phi}_A \times \mathbf{Q}_{AA} = \boldsymbol{\phi}_B\mathbf{Q}_{BB} = 0$ and $\boldsymbol{\phi}_A\tilde{\mathbf{Q}}_{AB}[S] = \boldsymbol{\phi}_B\mathbf{Q}_{BA}$ (see Sec. 3.1), we can verify that $w = \boldsymbol{\phi}_B\mathbf{Q}_{BC}$ is the solution, which does not depend on $[S]$. We thus know from Lemma 4.2 and (4.6) that $v = \chi[S]/([S] + C_M)$, where $\chi = \boldsymbol{\phi}_B\mathbf{Q}_{BC}\mathbf{1}/\{\boldsymbol{\phi}_B\mathbf{1}\}$ and $C_M = \{\boldsymbol{\phi}_B(\mathbf{Q}_{BA} + \mathbf{Q}_{BC})\tilde{\mathbf{Q}}_{AB}^{-1}\mathbf{1}\}/\{\boldsymbol{\phi}_B\mathbf{1}\}$.

Finally, consider Scenario 6. This scenario implies that $\mathbf{Q}_{BC} \propto \mathbf{Q}_{BA}$, say $\mathbf{Q}_{BC} = \kappa\mathbf{Q}_{BA}$. So $\mathbf{I} + \mathbf{Q}_{BC}^{-1}\mathbf{M}^{-1} = \mathbf{Q}_{BC}^{-1}\mathbf{Q}_{BB} - \mathbf{Q}_{BC}^{-1} \times (\mathbf{Q}_{BB} - (1+\kappa)\mathbf{Q}_{BA})\tilde{\mathbf{Q}}_{AB}^{-1}\mathbf{Q}_{AA}/[S]$. Using the facts that $\boldsymbol{\phi}_A\mathbf{Q}_{AA} = \boldsymbol{\phi}_B\mathbf{Q}_{BB} = 0$ and $\boldsymbol{\phi}_A\tilde{\mathbf{Q}}_{AB}[S] = \boldsymbol{\phi}_B\mathbf{Q}_{BA}$, we can verify that $\mathbf{w} = \boldsymbol{\phi}_B\mathbf{Q}_{BC}$ is the solution of $\mathbf{w}(\mathbf{I} + \mathbf{Q}_{BC}^{-1}\mathbf{M}^{-1}) = 0$. It does not depend on $[S]$. It, thus, follows from Lemma 4.2 and (4.6) that $v = \chi[S]/([S] + C_M)$, where $\chi = \boldsymbol{\phi}_B\mathbf{Q}_{BC}\mathbf{1}/\{\boldsymbol{\phi}_B\mathbf{1}\}$ and $C_M = \{\boldsymbol{\phi}_B(\mathbf{Q}_{BA} + \mathbf{Q}_{BC})\tilde{\mathbf{Q}}_{AB}^{-1}\mathbf{1}\}/\{\boldsymbol{\phi}_B\mathbf{1}\}$.

[Received January 2007. Revised May 2007.]

REFERENCES

Albery, W. J., and Knowles, J. R. (1976), "Free-Energy Profile for the Reaction Catalyzed by Triosephosphate Isomerase," *Biochemistry*, 15, 5627–5631.

Asbury, C., Fehr, A., and Block, S. M. (2003), "Kinesin Moves by an Asymmetric Hand-Over-Hand Mechanism," *Science*, 302, 2130–2134.

Atkins, P., and de Paula, J. (2002), *Physical Chemistry* (7th ed.), New York: W. H. Freeman.

Ball, K., Kurtz, T. G., Popovic, L., and Rempala, G. (2006), "Asymptotic Analysis of Multiscale Approximations to Reaction Networks," *Annals of Applied Probability*, 16, 1925–1961.

Chen, H., and Yao, D. (2001), *Fundamentals of Queueing Networks*, New York: Springer-Verlag.

Colquhoun, D., and Hawkes, A. G. (1981), "On the Stochastic Properties of Single Ion Channels," *Proceedings of the Royal Society London*, Ser. B, 211, 205–235.

Dorland, W. A. (2003), *Dorland's Illustrated Medical Dictionary* (30th ed.), Philadelphia: W. B. Saunders.

English, B., Min, W., van Oijen, A. M., Lee, K. T., Luo, G., Sun, H., Cherayil, B. J., Kou, S. C., and Xie, X. S. (2006), "Ever-Fluctuating Single Enzyme Molecules: Michaelis–Menten Equation Revisited," *Nature Chemical Biology*, 2, 87–94.

Fersht, A. (1985), *Enzyme Structure and Mechanism* (2nd ed.), New York: W. H. Freeman.

Flomembom, O., et al. (2005), "Stretched Exponential Decay and Correlations in the Catalytic Activity of Fluctuating Single Lipase Molecules," *Proceedings of the National Academy of Sciences of the United States of America*, 102, 2368–2372.

Fredkin, D., and Rice, J. (1986), "On Aggregated Markov Processes," *Journal of Applied Probability*, 23, 208–214.

Glasserman, P., Sigman, K., and Yao, D. (eds.) (1996), *Stochastic Networks: Stability and Rare Events*, New York: Springer-Verlag.

Hammes, G. G. (1982), *Enzymatic Catalysis and Regulation*, New York: Academic Press.

Heyde, C. C. (1997), *Quasi-Likelihood and Its Application*, New York: Springer-Verlag.

Jacobson, R. H., Zhang, X. J., DuBose, R. F., and Matthews, B. W. (1994), "Three-Dimensional Structure of β-Galactosidase From *E. coli*," *Nature*, 369, 761–766.

Keilson, J. (1979), *Markov Chain Models—Rarity and Exponentiality*, New York: Springer-Verlag.

Kelly, F. P. (1979), *Reversibility and Stochastic Networks*, New York: Wiley.

Kelly, F. P., and Williams, R. J. (eds.) (1995), *Stochastic Networks*, New York: Springer-Verlag.

Kijima, M. (1997), *Markov Processes for Stochastic Modeling*, London: Chapman & Hall.

Kou, S. C. (2008), "Stochastic Modeling in Nanoscale Biophysics: Subdiffusion Within Proteins," *Annals of Applied Statistics*, 2, 501–535.

Kou, S. C., and Xie, X. S. (2004), "Generalized Langevin Equation With Fractional Gaussian Noise: Subdiffusion Within a Single Protein Molecule," *Physical Review Letters*, 93, 180603(1)–180603(4).

Kou, S. C., Cherayil, B., Min, W., English, B., and Xie, X. S. (2005a), "Single-Molecule Michaelis–Menten Equations," *Journal of Physical Chemistry B*, 109, 19068–19081.

Kou, S. C., Xie, X. S., and Liu, J. S. (2005b), "Bayesian Analysis of Single-Molecule Experimental Data" (with discussion), *Journal of the Royal Statistical Society*, Ser. C, 54, 469–506.

Lewis, G. N. (1925), "A New Principle of Equilibrium," *Proceedings of the Natianal Academy of Sciences of the United States of America*, 11, 179–183.

Lu, H. P., Xun, L., and Xie, X. S. (1998), "Single-Molecule Enzymatic Dynamics," *Science*, 282, 1877–1882.

Min, W., English, B., Luo, G., Cherayil, B., Kou, S. C., and Xie, X. S. (2005a), "Fluctuating Enzymes: Lessons From Single-Molecule Studies," *Accounts of Chemical Research*, 38, 923–931.

Min, W., Gopich, I. V., English, B., Kou, S. C., Xie, X. S., and Szabo, A. (2006), "When Does the Michaelis–Menten Equation Hold for Fluctuating Enzymes?" *Journal of Physical Chemistry B*, 110, 20093–20097.

Min, W., Luo, G., Cherayil, B., Kou, S. C., and Xie, X. S. (2005b), "Observation of a Power Law Memory Kernel for Fluctuations Within a Single Protein Molecule," *Physical Review Letters*, 94, 198302(1)–198302(4).

Moerner, W. (2002), "A Dozen Years of Single-Molecule Spectroscopy in Physics, Chemistry, and Biophysics," *Journal of Physical Chemistry B*, 106, 910–927.

Nie, S., and Zare, R. (1997), "Optical Detection of Single Molecules," *Annual Review of Biophysics and Biomolecular Structure*, 26, 567–596.

Press, W., Flannery, B., Teukolsky, S., and Vetterling, W. (1992), *Numerical Recipes in C: The Art of Scientific Computing* (2nd ed.), New York: Cambridge University Press.

Schnakenberg, J. (1976), "Network Theory of Microscopic and Macroscopic Behavior of Master Equation Systems," *Reviews of Modern Physics*, 48, 571–585.

Segel, I. H. (1993), *Enzyme Kinetics: Behavior and Analysis of Rapid Equilibrium and Steady-State Enzyme Systems*, New York: Wiley.

Serfozo, R. (1999), *Introduction to Stochastic Networks*, New York: Springer-Verlag.

Tamarat, P., Maali, A., Lounis, B., and Orrit, M. (2000), "Ten Years of Single-Molecule Spectroscopy," *Journal of Physical Chemistry A*, 104, 1–16.

Weiss, S. (2000), "Measuring Conformational Dynamics of Biomolecules by Single Molecule Fluorescence Spectroscopy," *Nature Structural Biology*, 7, 724–729.

Xie, X. S., and Lu, H. P. (1999), "Single-Molecule Enzymology," *Journal of Biological Chemistry*, 274, 15967–15970.

Xie, X. S., and Trautman, J. K. (1998), "Optical Studies of Single Molecules at Room Temperature," *Annual Review of Physical Chemistry*, 49, 441–480.

Yang, H., Luo, G., Karnchanaphanurach, P., Louise, T.-M., Rech, I., Cova, S., Xun, L., and Xie, X. S. (2003), "Protein Conformational Dynamics Probed by Single-Molecule Electron Transfer," *Science*, 302, 262–266.

Yang, S., and Cao, J. (2001), "Two-Event Echos in Single-Molecule Kinetics: A Signature of Conformational Fluctuations," *Journal of Physical Chemistry B*, 105, 6536–6549.

Zhuang, X., Kim, H., Pereira, M., Babcock, H., Walter, N., and Chu, S. (2002), "Correlating Structural Dynamics and Function in Single Ribozyme Molecules," *Science*, 296, 1473–1476.